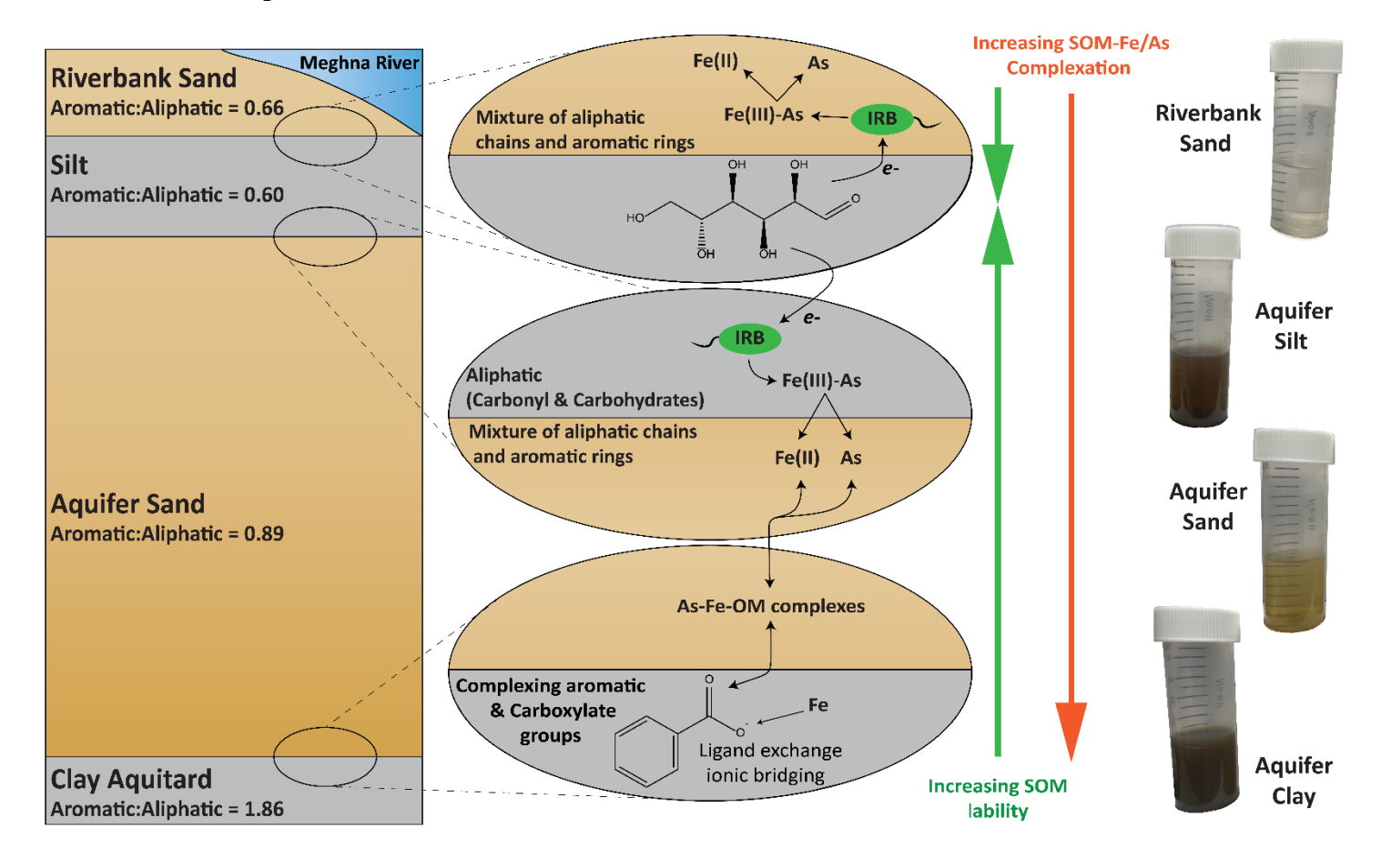
Diverse Sedimentary Organic Matter within the River-Aquifer Interface Drives Arsenic
Mobility along the Meghna River Corridor in Bangladesh
Thomas S. Varner <sup>1*</sup> , Harshad V. Kulkarni <sup>1,4*</sup> , Kyungwon Kwak <sup>2</sup> , M. Bayani Cardenas <sup>3</sup> , Peter S.K. Knappett <sup>2</sup> , Saugata Datta <sup>1*</sup>
<sup>1</sup> Department of Earth and Planetary Sciences, University of Texas at San Antonio, San Antonio, TX, 78249, USA
<sup>2</sup> Department of Geology and Geophysics, Texas A&M University, College Station, TX 77843,
USA
<sup>3</sup> Department of Geological Sciences, The University of Texas at Austin, TX 78712, USA
<sup>4</sup> School of Civil and Environmental Engineering, Indian Institute of Technology Mandi,
Himachal Pradesh, 175005, India.
Corresponding authors: Thomas S. Varner (tom.varner@my.utsa.edu), Harshad V. Kulkarni
( <u>harshad@iitmandi.ac.in / harshad.env@gmail.com</u> ), Saugata Datta ( <u>saugata.datta@utsa.edu</u> )
Highlights
1. Infrared spectroscopic analyses of sedimentary organic matter (SOM) from an arsenic
contaminated river-aquifer interface
2. Enrichment of polysaccharide and carbonyl functional groups in near-surface silt layer
3. Enrichment of carboxyl function groups in underlying clay aquitard
4. Labile SOM in the river-aquifer mixing zone promotes Fe and As mobility through reductive
dissolution of Fe-oxides
5. Recalcitrant SOM from clay aquitard promotes Fe and As mobility through complexation
Keywords: Sedimentary Organic Matter; Arsenic; Hyporheic zone; Functional groups;
Meghna River; Fourier Transform Infrared Spectroscopy.

# 30 Graphical Abstract



#### Abstract

31

32

33

34

35

36

37

38

39

40

41

42

43

44

45

46

47

48

49

50

51

52

In alluvial aquifers with near-neutral pH and high dissolved arsenic (As) concentrations, the presence and character of sedimentary organic matter (SOM) regulates As mobility by serving as an energetically variable source of electrons for redox reactions or forming As-Fe-OM complexes. Near tidally and seasonally fluctuating rivers, the hyporheic zone (HZ), which embodies the mixing zone between oxic river water and anoxic shallow groundwater, may precipitate (or dissolve) iron (Fe)-oxides which sequester (or mobilize) As. To understand what is driving the mobilization of As within a shallow aquifer and riverbank sands adjacent to the tidally fluctuating Meghna River, we characterized the chemical reactivity of SOM from the sands, and a silt and clay layer, underlying the HZ and aquifer, respectively. Dissolved As (50-500 µg/L) and Fe (1-40 mg/L) concentrations increase with depth within the shallow aquifer. Similar vertical As and Fe concentration gradients were observed within the riverbank sands where concentrations of the products of reductive dissolution of Fe-oxides increase with proximity to the silt layer. Compared to all other sediments, the SOM in the clay aquitard contains older, more recalcitrant, terrestriallyderived material with high proportions of aromatic carboxylate functional groups. The shallow silt layer contains fresher SOM with higher proportions of amides and more labile polysaccharide moieties. The SOM in both the riverbank and aguifer is terrestrially-derived and humic-like. The labile SOM from the silt layer drives the microbially mediated reductive dissolution of As-bearing Fe-oxides in the HZ. In contrast, the carboxylate-rich SOM from the clay aquitard maintains dissolved As concentrations at the base of the aquifer by complexing with soluble As and Fe. This highlights that SOM-rich fine (silt or clay) layers in the Bengal basin drive As and Fe mobility, however, the specific processes mobilizing As and Fe depend on the lability of the SOM.

#### 1 Introduction

53

54

55

56

57

58

59

60

61

62

63

64

65

66

67

68

69

70

71

72

73

74

75

Organic matter in sediments, referred to herein as sedimentary organic matter (SOM), plays a vital role in mobilizing arsenic (As) in the shallow Holocene aquifers of the Ganga-Meghna-Brahmaputra (GMB) delta (Nickson et al., 2000; McArthur et al., 2004; Mladenov et al., 2010; Mailloux et al., 2013). Elevated dissolved As concentrations in the aquifers of the GMB delta jeopardize the health of millions who rely on the groundwater for drinking purposes (Flanagan et al., 2012). This problem has been of global concern for decades, motivating many studies that have improved the understanding of the natural processes that generate dissolved As in reducing fluviodeltaic aquifers (Smith et al., 2000; BGS&DPHE, 2001; Mukherjee & Bhattacharya, 2001; Yu et al., 2003; Flanagan et al., 2012). Yet millions in the Bengal basin still consume groundwater that is contaminated with As. Despite the fact that OM has long been implicated in the release of As from sediments to the groundwater (Nickson et al., 2000), the specific role that molecularly diverse OM has on As mobilization and its interactions with microbes and minerals is not fully understood. The composition of OM varies greatly in terrestrial environments and is determined by its original source and exposure to biological metabolisms (Laspidou & Rittmann, 2002). In general, the majority of OM is composed of refractory humic substances (i.e. humic acid, fulvic acid and humin) (Piccolo, 1996; Senesi et al., 2003) and labile OM which consists of sugars, microbial byproducts, and protein-like components (i.e. amino acids) (Coble & Timperman, 1998; Yamashita & Tanoue, 2003; Borisover et al., 2012). Humic substances are generally characterized by a high molecular weight, chemical recalcitrance, and are composed of a complex and heterogeneous mixture of organic compounds. Humic substances typically contain between 40 -50% aliphatic components, which are classified as open carbon chains, and between 35 - 60% aromatic components, which are classified by a circular and planar molecular structure (Pettit,

2004). In contrast, the labile pool of OM is readily biodegradable, providing accessible electrons as a preferred energy source for microbial respiration (Haynes, 2005). Together, these refractory and labile OM components drive heterotrophic processes in the environment (McManus et al., 2003).

76

77

78

79

80

81

82

83

84

85

86

87

88

89

90

91

92

93

94

95

96

97

98

In the environment, OM participates in a variety of chemical reactions. Notably, the ability of OM to donate electrons allows for the rapid consumption of oxygen to drive reducing conditions (Aeschbacher et al., 2010; Macalady & Walton-Day, 2011; Wallace et al., 2017; Lv et al., 2018) and alter the surface reactivity of minerals (Qu & Cwiertny, 2013). A key reaction responsible for the release of As in aquifers is the microbially mediated reductive dissolution of As-bearing Feoxide minerals in the presence of labile OM (Nickson et al., 1998; Nickson et al., 2000; Bhattacharya et al., 2001; McArthur et al., 2001; Zheng et al., 2004; Hasan et al., 2007; Glodowska et al., 2020; Qiao et al., 2020; Vega et al., 2020). In contrast, recalcitrant humic substances may increase As mobility by competing with As for positively charged anionic sorption sites (Redman et al., 2002; Simeoni et al., 2003; Bauer & Blodau, 2006; Gustafsson, 2006; Wang & Mulligan, 2006; Xue et al., 2019). Recalcitrant humic substances may also form ternary As-Fe-OM complexes wherein Fe<sup>III</sup> stabilizes the complex by serving as a cationic bridge between the OM and As (Deng & Dixon, 2002; Ritter et al., 2006; Sharma et al., 2010; Liu et al., 2011; Hoffmann et al., 2013). In summary, whether reducing or blocking sorption sites, or stabilizing As in solution, OM plays a ubiquitous role in regulating the mobility of As and may be key to predicting the distribution of dissolved As in shallow reducing aquifers (Anawar et al., 2003; Mladenov et al., 2010; Anawar et al., 2013).

The specific role that OM plays in the mobilization of As depends largely on the chemical makeup of the OM. The chemical makeup is related to the OM source such as buried detrital OM

and advected DOM, however, the source of the OM driving As mobilization in the aquifers of Bangladesh remains uncertain (Mailloux et al., 2013). Several hypotheses have been tested on data from detailed investigations on the source of OM driving this reaction in the shallow aquifers. For example, the following sources of OM have been hypothesized to promote the reductive dissolution of As-bearing Fe-oxides: 1) the downward advection of dissolved organic matter (DOM) from surface water (Harvey et al., 2006; Neumann et al., 2010); 2) DOM leached from buried silt, peat, or clay lenses (McArthur et al., 2001; McArthur et al., 2004; Ravenscroft et al., 2005); or 3) DOM leached from detrital OM buried in aquifer sediments (Datta et al., 2011; Neumann et al., 2014). To understand where along a specific flow path within an aquifer that the reduction of Fe-oxides by OM mobilizes As into the porewaters, as opposed to competitive desorption or complexation processes, the chemical makeup of the SOM must be measured. Zones within aquifers where abundant Fe<sup>III</sup> and SOM co-occur, such as redox interfaces, are likely key locations where As is both mobilized and immobilized under the influence of SOM, although only the net mass flux of As between the dissolved and solid-phase can be observed (Berube et al., 2018; Jewell et al., 2023). Ultimately, the geochemical cycling of OM, Fe, and As are tightly linked and redox interfaces have been implicated in acting as intermediate barriers that limit the transportation of these elements (Charette & Sholkovitz, 2002; Datta et al., 2009; Riedel et al., 2013). One widely prevalent redox interface is the hyporheic zone (HZ) within riverbank sediments lining rivers. In the HZ, fluctuating redox conditions support a diverse microbial community which can effectively metabolize OM to create a biogeochemical hotspot with enhanced chemical

reaction rates relative to adjacent areas (Fiebig, 1995; Findlay et al., 2003; Fischer et al., 2005;

Nogaro et al., 2013; Shuai et al., 2017a; Zhu et al., 2020; Xia et al., 2023). The high rates of OM

99

100

101

102

103

104

105

106

107

108

109

110

111

112

113

114

115

116

117

118

119

120

metabolization within the HZ are sustained by fluctuating redox conditions, the advective and dispersive transport of oxidants and reductants, temperature gradients, and a continuous source of OM introduced by the infiltrating river water (Burrows et al., 2017; Shuai et al., 2017a; Stegen et al., 2023). Along the Meghna River in Bangladesh, As tends to be immobilized in the riverbank, and therefore, over time, accumulates in the HZ up to 23,000 mg/kg (Datta et al., 2009; Berube, 2017; Berube et al., 2018). In this setting, reduced groundwater, rich in dissolved Fe<sup>II</sup> and As advects towards the river and mixes with the oxic river water under vigorous tidal fluctuations (Datta et al., 2009; Jung et al., 2012; Jung et al., 2015; Berube et al., 2018; Varner et al., 2022). In sufficiently permeable sediments, the two waters interact to precipitate amorphous Fe-oxides which then immobilize As on surface sorption sites (Datta et al., 2009; Jung et al., 2015; Berube et al., 2018; Huang et al., 2022). The propensity of OM to donate electrons for the microbial reduction of these Fe-oxides, or to form As-Fe-OM complexes, makes the characterization of OM a necessary component in understanding the causes of the observed mass fluxes of As between the dissolved- and solid-phases across these redox interfaces (Jewell et al., 2023; Kwak et al., In Revision). Our recent work along the Meghna River (Varner et al., 2022) revealed that the riverbank sands contained low concentrations of solid-phase As (<10 mg/kg) compared to other nearby sandy riverbank locations (>100 mg/kg) (Datta et al., 2009; Jung et al., 2012; Jung et al., 2015; Berube, 2017; Berube et al., 2018). The low solid-phase As concentrations at this new site may be attributed to a buried silt layer that may prevent Fe-oxide formation by impeding groundwater mixing and/or providing OM to the riverbank to sustain reducing conditions (Kwak et al., In Revision). This

hypothesis was supported by fluorescence observations by Varner et al. (2022) which suggested

the presence of highly labile OM in the water-extractable fraction of the SOM from the buried silt

122

123

124

125

126

127

128

129

130

131

132

133

134

135

136

137

138

139

140

141

142

143

layer and riverbank sands. Thus, labile OM from the silt layer may be transported by molecular diffusion and/or advection by upwelling groundwater, to provide sufficient labile OM for heterotrophic metabolisms in the riverbank sands. Therefore, we hypothesize that spectroscopically distinct SOM, identified by fluorescence spectroscopy, will contain chemically distinct functional groups, which interact in unique ways with As and Fe within the riverbank, and this interaction impacts their mobilization within the riverbank.

To our knowledge, the relationship between the specific chemical composition of SOM and As mobilization within sediments bordering a fluctuating river in the Bengal basin has not been examined. In this study, we define the structural characteristics of SOM from within an As contaminated aquifer and adjacent HZ sediments along the Meghna River utilizing both UV-Vis and FTIR spectroscopic techniques (Minor et al., 2014). We characterized the specific functional groups comprising the SOM to better constrain the reactivity of SOM and its relationship to As and Fe mobility across the steep redox gradient represented by the river-aquifer interface.

### 2 Methods

### 2.1 Study site

The study site lies along the Meghna River 30 km east of Dhaka, adjacent to the village of Nayapara (23.7°N, 90.7°E) within the Araihazar sub-district in the Narayanganj district (Fig. 1a). The lithology of the shallow aquifers (<60 m) in Araihazar are typical of fluvio-deltaic depositional environments, consisting of medium to fine unconsolidated sand with interbedded lenses of silt and clay (Aziz et al., 2008; Bibi et al., 2008; Weinman et al., 2008). The detailed lithology at this site along the Meghna River is described in Varner et al. (2022). Briefly, from bottom to top it consists of four units; an underlying clay layer at ~36 m below ground level (bgl), medium sands

which comprises the shallow aquifer between 36 and 7 bgl, a silt layer between 7 and 3 m bgl and finally a fine riverbank sand between 3 and 0 m bgl that hosts the HZ.

The co-occurrence of high dissolved As and Fe concentrations in the shallow aquifers underneath the Meghna River floodplain have been well documented (BGS&DPHE, 2001; van Geen et al., 2003; van Geen et al., 2014). Along the Meghna River shallow groundwater flows towards the river for most of the year (Huang et al., 2022), and multiple studies have observed high solid-phase concentrations of As (>100 mg/kg) and Fe (>30,000 mg/kg) within the HZ sediments (Datta et al., 2009; Jung et al., 2012; Jung et al., 2015; Berube et al., 2018). This suggests that advected As and Fe from the shallow aquifer may accumulate in the HZ under the influence

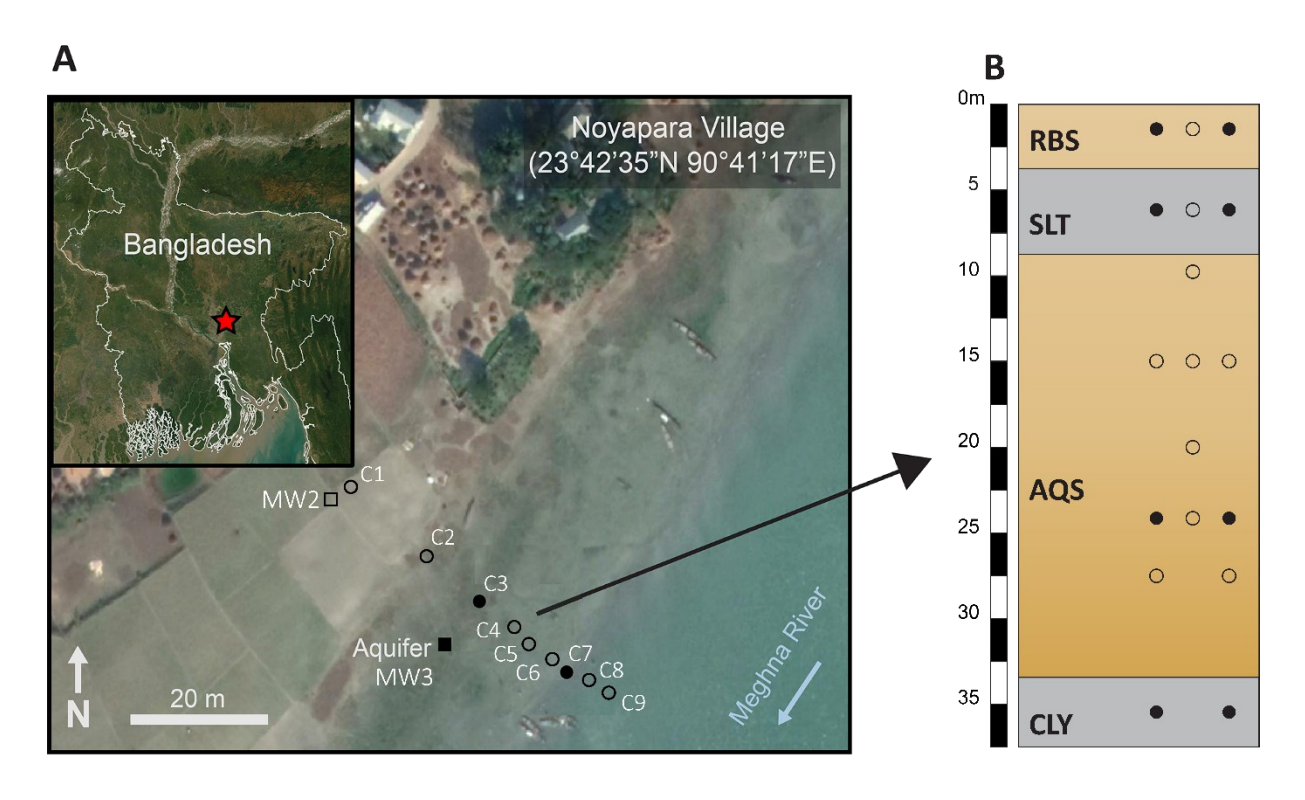


**Figure 1.** (A) Map of study site with sampling locations (adopted from Varner et al., 2022) of riverbank sediment (circles) and aquifer sediment (squares). The filled symbols represent the sampling locations of the sediment used in this study. (B) Depiction of the subsurface lithology at the site derived from an electrical resistivity transect along the riverbank and drill cuttings from the aquifer borehole (Pedrazas et al., 2021; Varner et al., 2022). The riverbank sand, silt, aquifer sand, and clay layers are shown as RBS, SLT, AQS, and CLY, respectively. The filled symbols represent the sampling depths of the sediment used in this study, the open symbols represent additional sediment sample previously characterized for solid-phase and water-extractable properties in Varner et al. (2022).

of mixing with the oxygenated river water. This mixing is in turn driven by tidal and seasonal fluctuations in the river stage (Shuai et al., 2017b). During the dry season, the river is most strongly gaining. However, when the riverbank is inundated during the wet season, the river becomes weakly gaining or slightly losing (Berube et al., 2018; Huang et al., 2022).

## 2.2 Sample collection and analyses

176

177

178

179

180

181

182

183

184

185

186

187

188

189

190

191

192

193

194

195

196

197

198

The riverbank and aguifer sediment samples used in this study (n = 8) were collected from the study site along the Meghna River in January 2020. The aquifer sediment was collected as sediment cuttings from a borehole installed using the traditional hand flapper method (n = 6)(Horneman et al., 2004), whereas the surficial riverbank sediment (n = 2) was collected from a depth of 0.6 m bgl using a direct push sediment probe (AMS Inc., USA). Two representative samples from each lithology; riverbank sand (RBS, 0.6 m), buried silt (SLT, 6 m), aquifer sand (AQS, 23 m), and the underlying clay aguitard (CLY, ~35 m) were selected for this study (Fig. 1b). The average loss on ignition (LOI, a proxy for sedimentary carbon content) was determined to be 1.9 wt% for the RBS, 4.8 wt% for the SLT, 1.8% wt% for the AQS and 7.7% wt% for the CLY samples (Varner et al., 2022). Analyses of RBS (n = 32, from nine sediment cores), and the AQS (n = 13), SLT (n = 3), and CLY (n = 2) samples from three drill cuttings (Varner et al., 2022) showed that the spectroscopic properties of water-extractable SOM within the sample groups (e.g., RBS, AQS, SLT and CLY) were distinct from each other. Four well-characterized samples were selected from each group (RBS, SLT, AQS and CLY) to characterize the functional groups in detail. The elemental composition, particle size distribution, and spectroscopic properties of waterextractable organic matter of these samples were described in Varner et al. (2022). All sediment samples used in this study were stored in Mylar Remel® bags with an O2 absorbent pouch in the field and kept at -7 °C until analysis.

## 2.3 Sedimentary organic matter (SOM) extraction using NaOH

To extract the SOM from the riverbank and aquifer sediments, 2.5 g of air-dried sediment was powdered using an agate mortar and pestle and placed in a 50 ml centrifuge tube with 25 ml of 0.1 M NaOH solution (pH = 10.6). The mixture was mechanically shaken for 20 h (table shaker, 60 rpm) at ambient temperature. The supernatant was separated from the solid phase by centrifugation (12,000 rpm, 20 min). Following centrifugation, the supernatant of the NaOH extractant solution was 0.45  $\mu$ m filtered and immediately lyophilized for FTIR measurement to avoid any loss or degradation of the OM in solution (Lin, 2015; Sandron et al., 2015).

In Varner et al. (2022), the SOM from these samples was extracted using ultrapure water and analyzed using UV-Vis absorbance and fluorescence spectroscopy, and the approximate molecular weight was determined by size exclusion chromatography. The water extractable SOM, however, only represents the water soluble or most bioavailable pool of SOM in the samples (Zhao et al., 2022), however, this procedure does not account for all the SOM in the sample. Therefore, in this study a more aggressive extraction procedure using NaOH is used to extract bulk SOM from the samples and subsequently characterize its molecular properties. Extractions using NaOH have been widely used to extract natural SOM (Stevenson, 1994). Acidification of the NaOH extracts allows for the selective partitioning of humic and fulvic acids from the solution (Bai et al., 2020). In this study, however, the extract solutions were not acidified to retain all humic and non-humic fractions of the SOM. Such NaOH extractions have been shown to release a large percentage of the SOM and include not only humic substances, but also the low molecular weight acids, protein-like substances, and saccharide derivatives which comprise between 25 - 35% of the overall SOM in inorganic soils (Schnitzer, 1983; Ping et al., 2001).

### 2.4 Spectroscopic characterization of NaOH extractable organic matter

The mid-infrared spectra of the lyophilized NaOH sediment-extracts and a standard humic acid (HA) material (Sigma Aldrich humic acid, Aldrich Chemical Co., Product No. H16752) were obtained by attenuated total reflectance Fourier-transform infrared spectroscopy (ATR-FTIR) over the 4000-650 cm<sup>-1</sup> range on a Shimadzu IRSpirit spectrometer (Shimadzu Corporation, Japan). The spectrometer was fitted with a QATR-S diamond crystal attachment and a germanium-coated KBr beam splitter. Data were obtained as absorbance [log(1/reflectance)] and 64 scans at a resolution of 4 cm<sup>-1</sup> were averaged to obtain each sample spectrum. Background readings were collected between samples and subtracted from the subsequent measurements. The collected FTIR spectra were processed, baseline corrected, and smoothed in Spectragryph (v1.2.16.1).

To further characterize the spectroscopic properties of SOM, simultaneous UV-Vis measurement of the absorbance between 240 - 450 nm and the fluorescence between 300 - 600 nm was collected on the extract solutions using a benchtop fluorometer (Aqualog, Horiba). The measurement of the absorbance and fluorescence between these wavelengths encompasses the known range within which organic molecules absorb and emit, respectively. Following the methods described in Kulkarni et al. (2017), the spectroscopic data from the absorbance and fluorescence wavelengths were used to generate an excitation-emission matrix (EEM) for each sample.

Specific parameters were calculated from the UV-Vis spectroscopic data to provide further characterization of the source and dynamic processes of the SOM. The absorbance at 254 nm (abs254) is used as an indicator of the aromatic content of humic substances due to their high absorptivity at 254 nm (Weishaar et al., 2003; Wei et al., 2009; Batista et al., 2016). The humification index (HIX) provides an indication of the degree of humification (Ohno, 2002) and

is determined by the ratio of the emission (em) spectra peak area between 435 - 480 nm to the peak area between 300 - 345 nm at an excitation wavelength of 254 nm (Zsolnay, 2003). At 310 nm, an indication of recently produced SOM ( $\beta$ ) is observed along an emission of 380 nm, whereas more decomposed SOM ( $\alpha$ ) is observed by the maximum emission intensity between 420 - 435 nm (Parlanti et al., 2000). Together, the ratio of freshly produced SOM to decomposed SOM provides the freshness index ( $\beta$ : $\alpha$ ) (Huguet et al., 2009; Wilson & Xenopoulos, 2009; Fellman et al., 2010). The fluorescence index (FI) is the ratio of the emission intensities between 470 and 520 nm at an excitation of 370 nm, and provides an indication of whether the OM is terrestrially sourced (FI < 1.4) or microbially produced (FI > 1.7) (McKnight et al., 2001).

Furthermore, the assignment of peaks at established excitation/emission (ex/em) pairs for the peak-picking method is useful for characterizing and monitoring the organic properties in spectroscopic data (Goldman et al., 2012; Chen & Yu, 2021). For this study, commonly used ex/em pairs in the fluorescence spectra which reflect the structures present in the OM were used, including humic-like (peak A, 260/380 – 460 nm), fulvic-like (peak C, 320 – 260/420 – 460 nm), microbially derived (peak M, 290 – 310/370 – 410 nm), protein-like tryptophan (peak T, 270/340 nm), and protein-like tyrosine (peak B, 270/305 nm) (Coble et al., 1998; Coble et al., 2014).

The drEEM toolbox (v 0.6.0) was used for parallel factor analysis (PARAFAC) modeling. To meet the statistically significant number of samples to develop and validate the model, we included a previous dataset of 93 samples which included groundwater (n = 22), riverbank porewater (n = 20), river water (n = 3), and sediment-water extracts (n = 48) from the same location (Table S1) (Varner et al., 2022). The EEMs used to build this model were corrected following the protocol described in Murphy et al. (2013). Out of total of 97 samples used to build the model, one was found to be an outlier and was removed from the sample set. A three-component model using the

remaining 96 samples was validated by a split-half analysis of 50 models with three components, which confirmed the reliability of the three-component model through random initialization techniques. The proportion of each fluorophore component identified in the model for each sample is described in Figure S3 and Table S1. The EEMs of four samples used in this study (RBS, SLT, AQS and CLY) were fitted to this model to obtain respective proportions of fluorophores in these samples.

### 3 Results

## 3.1 Functional group assignments and variations in SOM

The FTIR spectra provided diagnostic information on the functional groups present in the SOM (Fig. 2). The assignment of functional groups was performed by comparing the sample spectra to previously reported ranges for common functional groups in natural waters and sediments (Table 1). Because some signals may overlap in the FTIR spectra, we confirmed the peak assignments by identifying co-occurring signals in the sample spectra for the correct assignment of specific functional groups (i.e., aliphatic CH shows peaks at both ~1450 cm<sup>-1</sup> for deformation and ~2920 cm<sup>-1</sup> for stretching). The possible effects from alkaline extraction on the SOM were also considered for the assignment of functional groups in the spectra. A more detailed description of peak assignments is provided in the supplementary text and the normalized FTIR spectra are shown in Figure S1 for comparison of relative peak sizes. Overall, the FTIR spectra for the NaOH extracts show IR absorptions that are typical for alkaline soil extracts (Oren & Chefetz, 2012).

The FTIR spectra of the CLY sample showed notable differences in the location and intensities of peaks in comparison to the peaks observed in RBS, SLT, and AQS (Fig. 2b). The absorbance band typically attributed to various O–H stretches in the CLY spectra was centered at

3360 cm<sup>-1</sup> and contained an additional peak at 3230 cm<sup>-1</sup>. A free O–H peak should occur at 3600 cm<sup>-1</sup>, however, the O–H stretch at 3360 cm<sup>-1</sup> reflects the dipole-dipole attraction of hydrogen-bonded O–H, whereas the peak at 3230 cm<sup>-1</sup> reflects the increased contributions from the N–H stretch of amides. Furthermore, relative to the other samples, the CLY spectrum showed a higher absorbance due to aromatic C–H stretching between 3100 - 3030 cm<sup>-1</sup>. In the 1800 - 1500 cm<sup>-1</sup> range, the CLY spectrum was similar to the spectra of the other samples, however, CLY contained a dominant peak at 1395 cm<sup>-1</sup>. The downward shift of this peak to slightly lower wavenumbers than that of the other sample spectra (~1440 cm<sup>-1</sup>) indicates lower absorbance from aliphatic C–H deformation and drastically higher absorbance from C–O stretching of carboxylic derivatives (i.e., sodium benzoate) and asymmetric COO<sup>-</sup> stretching. In comparison to the other samples, CLY shows only minor absorbance between ~1180 - 1000 cm<sup>-1</sup> and a relatively small peak at 880 cm<sup>-1</sup>

bending of aromatic C–H, respectively.

Table 1. Functional group assignments for specific bands and peaks observed within the mid-infrared wavelengths.

Absorption (cm <sup>1</sup> )	FTIR band	Assignment	Reference	
3700-3300	O–H bonds	Unresolved: phenol, alcohol, carbohydrates, COOH, Si-O-H in clay minerals, N-H stretch	1-15	
3100-3030	Aromatic C-H stretch	Aromatic stretch of highly substituted rings in HA macromolecules	1, 2, 5, 9, 12, 16	
2970-2820	Aliphatic C-H Stretch	Aliphatic C–H stretch of CH <sub>2</sub>	1-13, 16-20	
1720-1700	C=O stretch	Protonated carboxylic acid: aliphatic	2-4, 6, 7, 10-15, 18, 19, 21-25	
1670-1630	C=O stretch	Aliphatic carbonyl structures including proteinaceous amide I, conjugated ketones, and quinone-like compounds	1-7, 9-11, 13-15, 18- 25	
1630-1600	Aromatic C=C stretch	Aromatic ring stretch. May indicate ternary As-Fe-OM complexes	3-8, 10, 15, 19, 20	
1570-1550	Aromatic C=C stretch	Possible contribution from asymmetric COO- stretches	1-3, 8, 15, 16, 23, 26	
1515-1490	Aromatic C=C stretch	Possible contribution of amide N-H stretch	1, 4, 5, 7-11, 15, 16, 18-20, 23	
1470-1430	C-H deformation	Aliphatic C-H deformation	1, 2, 4, 5-9, 14-19, 21-23, 26	
1420-1370	Symmetric C-O Stretch	Aromatic carboxylate derivatives. Indicative of Na <sup>+</sup> salts (i.e., sodium benzoate)	1, 5-7, 11, 15, 17-19, 21-27	
1185-975	C—O—C and C—O—H stretching	Carbohydrates: aliphatic polysaccharide moieties	2, 4, 5-8, 11, 15, 19, 20, 26	
900-860	C-H out-of-plane bend	C-H bend of aromatic rings	1, 3, 5, 9, 15, 17, 18, 20, 23	

<sup>1.</sup> Bellamy (2013) 2. de Melo Benites et al. (2005) 3. Fultz et al. (2014) 4. Fernández-Getino et al. (2010) 5. Senesi et al. (2003) 6. Olk et al. (2000) 7. Chefetz et al. (1998) 8. Sánchez-Monedero et al. (2002) 9. Tatzber et al. (2007) 10. MacCarthy and Rice (1985) 11. Lumsdon and Fraser (2005) 12. Mecozzi and Pietrantonio (2006) 13. Litvin and Minaev (2013) 14. Reddy et al. (2018) 15. Minor and Stephens (2008) 16. Bustin and Guo (1999) 17. Oren and Chefetz (2012) 18. Nuzzo et al. (2020) 19. Guggenberger et al. (1994) 20. Peuravuori and Pihlaja (2004) 21. Mayo et al. (2004) 22. Chalmers and Griffiths (2002) 23. Ascough et al. (2011) 24. Stevenson (1994) 25. Hay and Myneni (2007) 26. Ilani et al. (2005) 27. Pike et al. (1993)

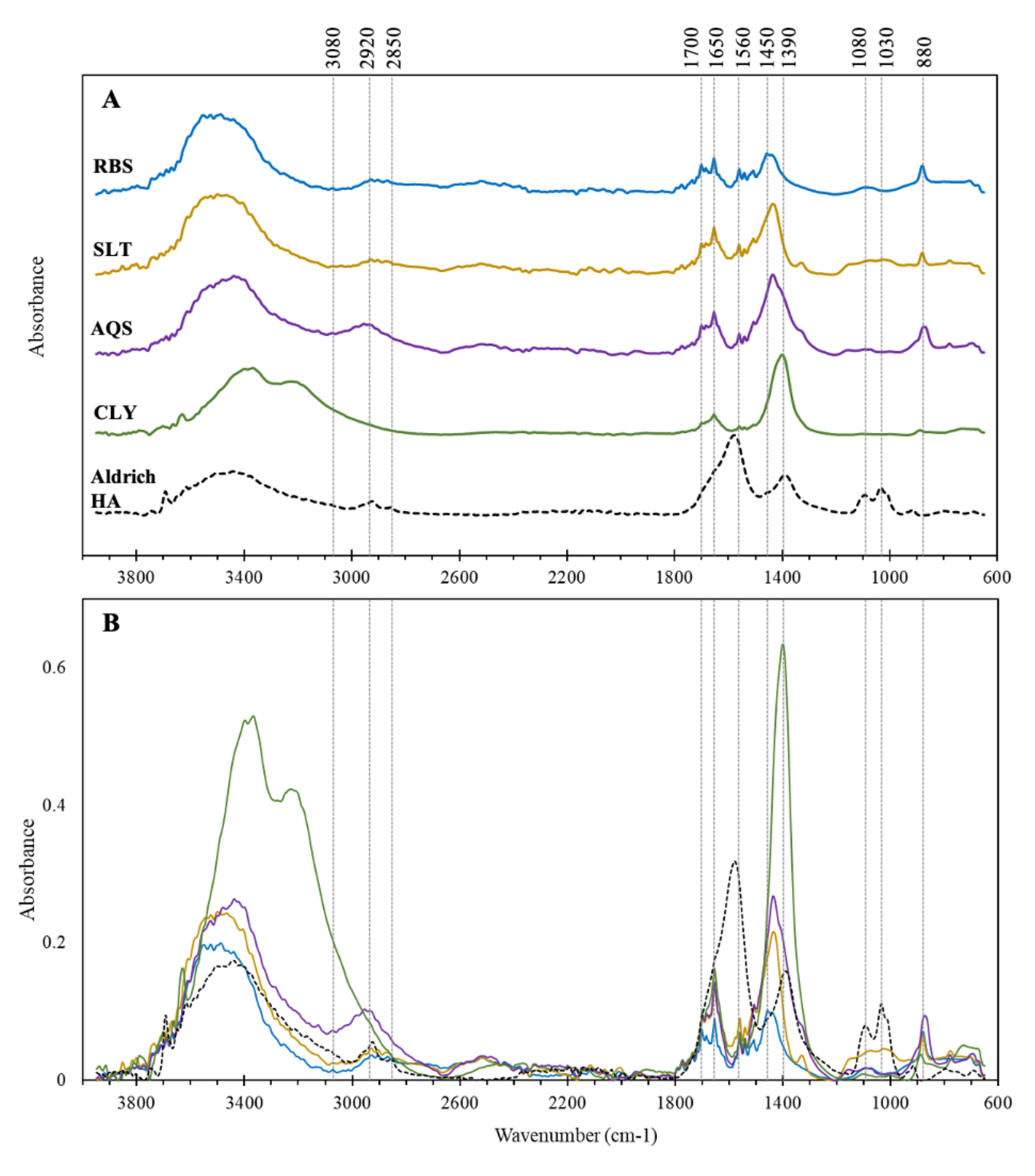


**Figure 2.** FTIR spectra of the lyophilized NaOH sediment extracts and Sigma Aldrich humic acid. The top panel shows normalized and stacked spectra (A) and the bottom panel shows all sample spectra together for comparison of peak intensities among the samples (B). The riverbank sand, silt, aquifer sand, and the clay aquitard are denoted by RBS, SLT, AQS, and CLY, respectively.

### 3.2 Distribution of functional groups in sedimentary organic matter

304

305

306

307

308

309

310

311

312

313

314

315

316

317

318

319

320

321

322

323

324

325

The relative contribution of each of the assigned functional groups to the overall sample SOM were estimated by taking the area under the peak between the wave numbers assigned to each functional group (Table 2). The FTIR spectra of the lyophilized NaOH extracts were compared to the standard Sigma Aldrich HA (Fig. 2a). The HA displayed prominent peaks at ~3400, 1590, 1390, and between 1100 - 1030 cm<sup>-1</sup>, which are typical for Sigma Aldrich HA, and are attributed to O–H stretches, aromatic C=C stretching, symmetric C–O stretching of carboxylic groups, and polysaccharide moieties, respectively (Guan et al., 2006; Liu et al., 2015). Based upon the peak assignments and known structure of the functional groups (Table 1) (Li et al., 2015), the aromaticity (a measurement of molecules that are both cyclic and planar) of the Sigma Aldrich HA was determined to be 56%, which is consistent with previously reported values (Kobayashi & Sumida, 2015) and is comparable to that of the <sup>13</sup>C nuclear magnetic resonance estimates for the International Humic Substances Society's standard HA (Thorn et al., 1989). The aromaticity of the SOM in the samples ranged between 40 - 65%. The major functional groups contributing to the SOM observed in the samples were aromatic rings (C–H at 3100 - 3030 and 900 - 860 cm<sup>-1</sup>; C=C stretch at 1630 - 1600, 1570 - 1550, and 1515 - 1490 cm<sup>-1</sup>), aliphatic C-H (2970 - 2820 and 1470 - 1430 cm<sup>-1</sup>), carbonyl (1670 - 1630 cm<sup>-1</sup>), protonated carboxyl groups (1720 - 1690 cm<sup>-1</sup>), deprotonated carboxyl groups attached to an aromatic ring (aromatic carboxylate groups, 1420 - 1370 cm<sup>-1</sup>), and carbohydrate (1180 - 1000 cm<sup>-1</sup>) (Fig. 3). Results show that the RBS, SLT, and AQS had similar aromatic to aliphatic (Ar:Al) ratios (0.66, 0.60, 0.89, respectively), whereas CLY had a much higher Ar:Al (1.86) (Fig. 3). The primary reason for a

markedly high Ar:Al in CLY is the large contribution of aromatic carboxylate structures (1420 -

1370 cm<sup>-1</sup>) in the spectrum (36%), which gradually increased with depth in each of the overlying RBS, SLT, and AQS samples (12%, 13%, and 19%, respectively) (Table S2).

One effect of alkali extractions is the deprotonation of dissociable carboxylic acid groups, which diminish the COOH absorbance bands in the FTIR spectra between 1720 - 1700 cm<sup>-1</sup>, and increase absorbance between 1400 - 1370 cm<sup>-1</sup> (Hay & Myneni, 2007; Nuzzo et al., 2020). These bands are commonly attributed to the carboxyl groups of sodium benzoate, which increase along with rising pH (Hayes et al., 1989; Guan et al., 2006; Lee & Seo, 2014). A comparison of the peaks at ~1720 and ~1400 cm<sup>-1</sup> suggests that most of the carboxyl groups in the SOM of all samples were deprotonated. The accumulation of simple compounds, such as benzene and carboxylate derivatives, with depth infer a higher level of humification. The increasing amounts of aromatic carboxylate groups (i.e., sodium benzoate) with depth indicates that the CLY contains a much more degraded (i.e., humified) pool of SOM (Fig. 2b, Table 2).

The proportions of aliphatic C–H were found to be higher in RBS (37%) and AQS (37%) than in the finer grain SLT (32%) and CLY (26%) samples (Fig. 3). However, neither grain size nor depth could solely explain the distribution of functional groups in the SOM as SLT contained a relatively large amount of carbohydrates (17%) but only trace amounts were present in CLY (<1%). Relative proportions of carbohydrates in the RBS and AQS were 9% and 5%, respectively. The proportions of the peaks assigned strictly to aromatic rings were comparable among RBS, SLT, AQS and CLY (28%, 25%, 28% and 29%, respectively), whereas carbonyl groups were found in slightly higher proportions in the RBS, SLT, and AQS (9%, 9%, 7%, respectively), than CLY (6%).

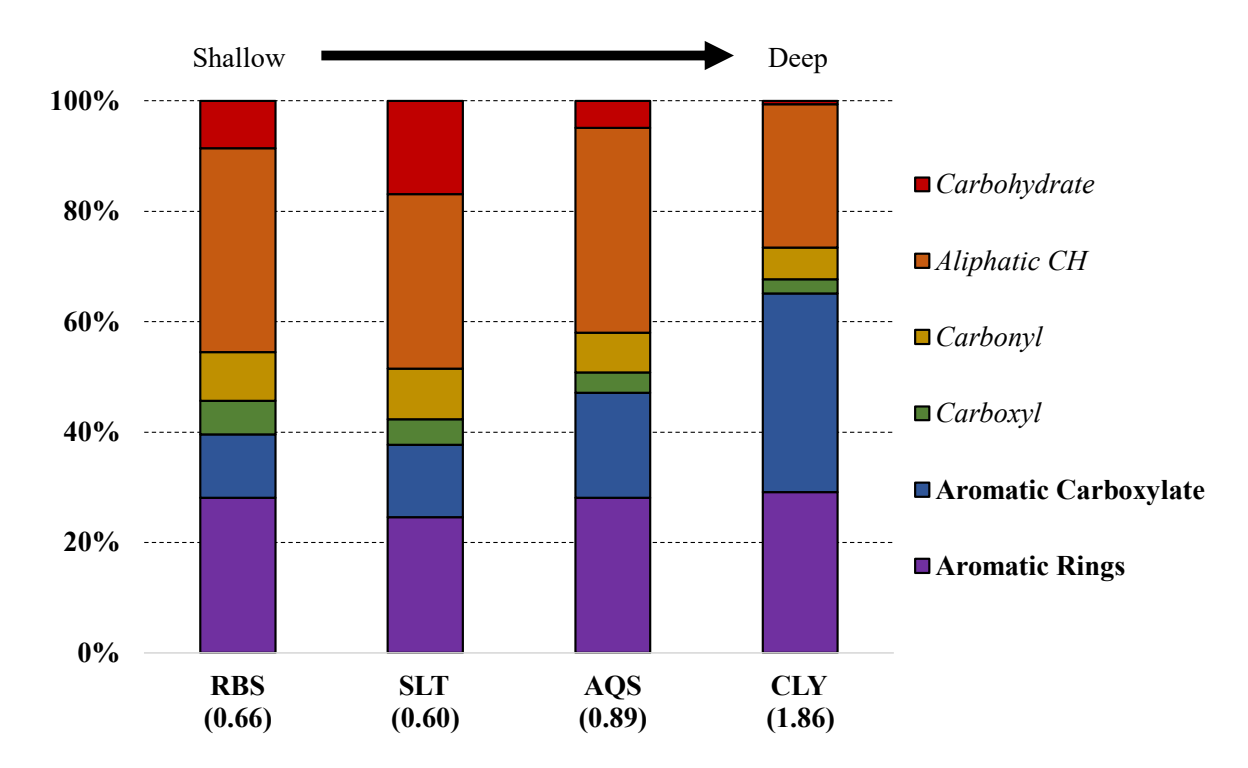


**Figure 3.** Proportions of functional groups in the sediment samples. **Bold** font represents groups attributed to aromatic structures and *Italicized* font represents groups attributed to aliphatic structures (Li et al., 2015). Value in parenthesis is the Ar:Al for each sample. The riverbank sand, silt, aquifer sand, and the clay aquitard are denoted by RBS (LOI = 1.9 wt%), SLT (LOI = 4.8 wt%), AQS (LOI = 1.8 wt%), and CLY (LOI = 7.7 wt%), respectively.

**Table 2.** Area under the peak for the assigned functional groups in the FTIR spectra of the samples and a standard humic acid, Sigma Aldrich humic acid (HA). The riverbank sand, silt, aquifer sand, and the clay aquitard are denoted by RBS, SLT, AQS, and CLY, respectively.

Sample	-	Carboxyl	Carbonyl			Carbohydrate		
	CH			Ring	Carboxylate		Area	Aliphatic
RBS	10.92	1.80	2.62	8.31	3.41	2.55	29.60	0.66
SLT	15.43	2.25	4.48	11.97	6.41	8.23	48.77	0.60
AQS	22.31	2.23	4.34	16.95	11.46	2.98	60.28	0.89
CLY	23.79	2.38	5.28	26.72	33.01	0.59	91.78	1.86
Aldrich HA	10.34	11.43	3.38	37.07	-	11.29	73.51	1.26

#### 3.3 Fluorescence characteristics of SOM

348

349

350

351

352

353

354

355

356

357

358

359

360

361

362

363

364

365

366

367

368

369

In addition to the FTIR results, the absorbance and fluorescence of the aqueous NaOH extracts provide further characterization of the SOM properties which may impact geochemical processes in the riverbank and aquifer (Fig. 4). The SOM in each layer, RBS, SLT, AQS, and CLY is terrestrially sourced (FI = 1.35, 1.32, 1.44, and 1.27, respectively). The age of the SOM is reflected by the freshness index which shows that the SOM within RBS and SLT ( $\beta$ : $\alpha = 0.73$  and 0.82, respectively) is more recently produced relative to the more degraded SOM found in the AQS and CLY ( $\beta$ : $\alpha$  = 0.53 and 0.63, respectively) (Table S3) which concurs with the depositional history. The presence of aromatic structures, as indicated by the absorbance at 254 nm (abs254), was elevated in CLY (abs254 = 11.07) relative to RBS, SLT, and AQS (abs254 = 1.33, 1.52, and 0.79, respectively). Four primary peaks were identified in the excitation and emission spectra of the samples for the peak-picking method (Table S3, Fig. 4), including; peak A (terrestrial humic-like), peak T (protein-like), peak C (terrestrial fulvic-like), and peak M (microbially produced, humic-like) (Coble et al., 1998). The peak typically attributed to tyrosine protein-like fluorescence (peak B) was not present in any of the samples. In general, the fluorescence indices show that SOM in all

the peak-picking method (Table S3, Fig. 4), including; peak A (terrestrial humic-like), peak T (protein-like), peak C (terrestrial fulvic-like), and peak M (microbially produced, humic-like) (Coble et al., 1998). The peak typically attributed to tyrosine protein-like fluorescence (peak B) was not present in any of the samples. In general, the fluorescence indices show that SOM in all samples is composed largely of humic and fulvic-like compounds (60 - 70%) with varying proportions of protein-like (1 - 7%) and microbially produced compounds (29 - 35%). The proportions represented by each peak were similar among each the samples, ranging between 43 - 48%, 17 - 19%, 29 - 35%, and 1 - 7% for peaks A, C, M, and T, respectively. However, the highest proportions of protein-like and microbially produced SOM are observed in the SLT as shown by a lower humic:protein ratio (humic:protein = 6.1) and a higher microbial:terrestrial ratio (peak

M/peak C = 2.0) compared to the RBS (9.2 and 1.68), AQS (24.0 and 1.83), and CLY (9.0 and 1.45) (Table S3).

The absorbance and fluorescence data complemented the FTIR results and provided further characterization of the SOM in the riverbank and aquifer sediments. Variations in SOM reactivity can be visualized by comparing the humic and fulvic-like signatures (peak A and C) with the protein-like and microbially produced SOM (peaks T and M) as it relates to the distribution of functional groups. For example, the sum of peaks T and M were positively correlated with the proportions of carbohydrate (r = 0.95) and carbonyl (r = 0.84) in the SOM, whereas the sum of peaks A and C are positively correlated with aromatic rings (r = 0.95) (Fig. S2).

The Ar:Al obtained from the assignment of the functional groups showed a positive association with both the humification index (HIX, r=0.78) and abs254 (r=0.96), which in turn were each negatively correlated with the proportions of aliphatic CH (r=-1.00 and -0.90, respectively) and positively correlated with the proportions of aromatic carboxylate (r=0.77 and 0.94, respectively) (Fig. S2). Fulvic-like SOM showed positive correlation with aromatic rings (peak C, r=0.98) whereas humic-like SOM was more closely associated with the aromatic-carboxyl structures (peak A, r=0.90). The relative proportions of humic-like SOM were negatively correlated with those of carbonyl and carbohydrates (r=-0.87, and -0.88, respectively). Conversely, the proportions of carbonyl and carbohydrate functional groups in the SOM were

positively correlated with  $\beta$ : $\alpha$  (r = 0.72 and 0.80, respectively) and the Microbial:Terrestrial ratio (r = 0.73 and 0.83, respectively). However, the relative proportions of carbonyl functional groups were more closely related to microbially produced SOM (peak M, r = 0.57) whereas the proportion of carbohydrates were associated with the proportions of protein-like SOM (r = 0.68). While these correlations provide valuable insights between the spectroscopic properties and functional group

distributions, their statistical significance shall be interpreted with caution because of the limited number of samples analyzed in this study. Although the potential heterogeneity in the individual sample type was not addressed in this study, the functional group distribution among four types of samples (RBS, SLT, AQS and CLY) is clearly distinguishable.

The PARAFAC model validated three components (Fig. S3) utilizing the 96 sample dataset comprised samples from this study (n = 4) and the water samples and sediment-water extracts from previous work at the same site (Varner et al., 2022) along the Meghna River (n = 92). The samples included in the PARAFAC model from this study were the NaOH sediment-extracts and differed from the remaining 92 samples, which were all measured for UV-Vis properties in a water-based medium. Despite showing a similar proportion of components, the NaOH extracts from this study contained much higher component values, specifically for component 1, compared to the water and sediment-water extracts presented in Varner et al. (2022) (Table S1). Due to the lack of representation of similar sample types in the 96 sample PARAFAC model, we determined that the model is not the best representation of the OM characteristics for the four NaOH samples examined in this study. However, the components included in the model remain consistent regardless of sample type, therefore, we have included the model results in the supplementary information.

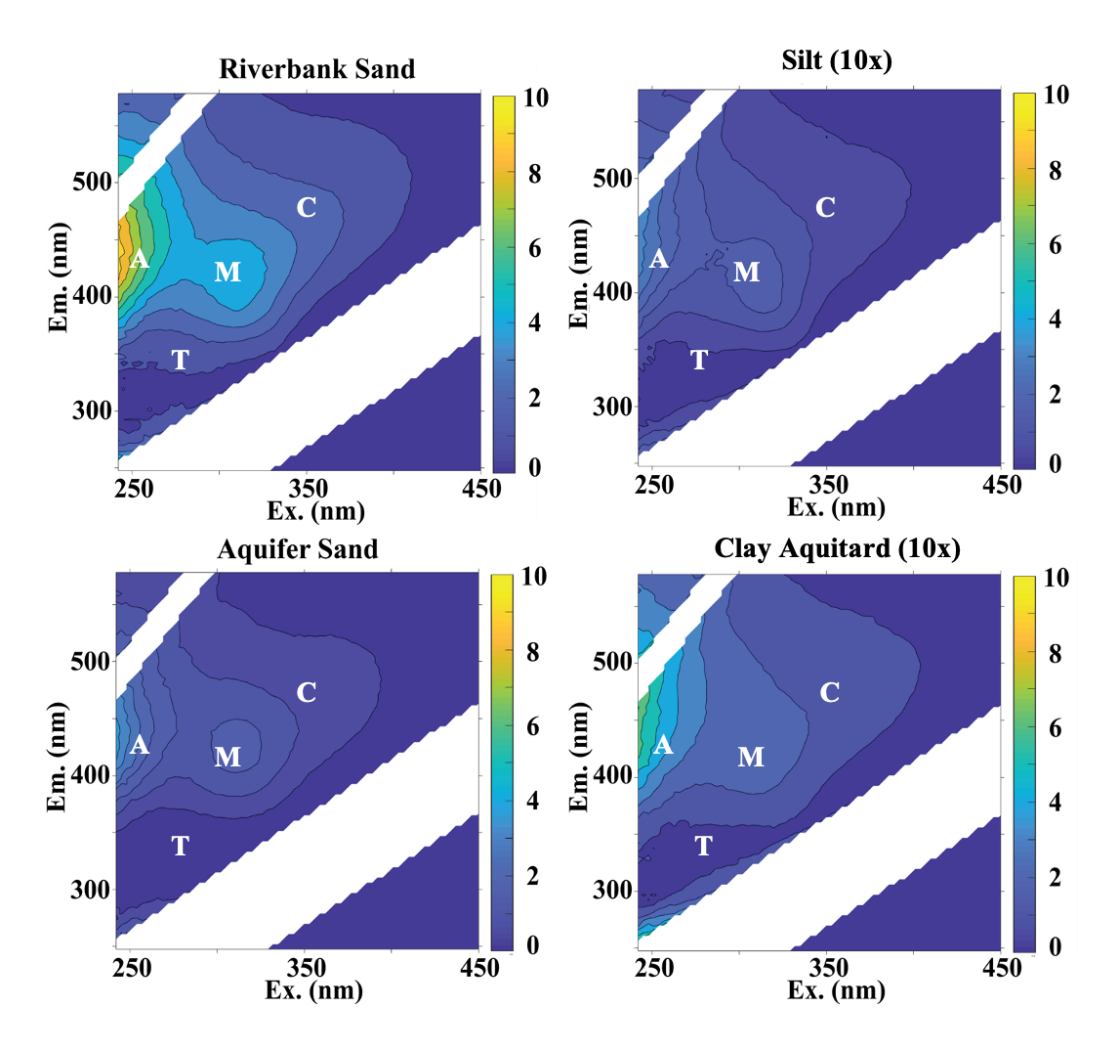


**Figure 4.** Excitation emission matrices of the samples. The silt and clay aquitard EEMs displayed are 10x diluted. All intensities are reported in Raman Unit (R.U.)

### 4 Discussion

410

411

412

413

414

415

416

417

418

419

420

421

422

423

424

425

426

427

428

429

430

431

## 4.1 Properties of SOM in the Aquifer and Riverbank sediments

The complimentary techniques used to characterize the spectroscopic properties of SOM revealed variations in its properties among the riverbank and aquifer sediments. In general, the positive relationship between the humification index (HIX) with the proportions of aromatic rings, aliphatic CH, and aromatic-carboxyl structures suggests that these functional groups are associated with more humified SOM which are enriched in AQS and CLY. Conversely, the younger, and more reactive SOM in the RBS and SLT contains higher proportions of both carbonyl and carbohydrates which are associated with protein-like and microbially produced SOM (Fig. 3, Table 2). Interestingly, sediment grain size is not a reliable indicator of the SOM properties. For example, the SOM from SLT and CLY contained contrasting proportions of functional groups, although their SOM did have a similar terrestrial source and a higher HIX than the sand samples. The SOM in the CLY was characterized by more degraded aromatic and carboxyl compounds of humic-acids and contained minimal proportions of labile OM such as carbohydrate (1%) and carbonyl groups (6%) (Fig. 3). The SOM in the SLT, on the other hand, showed higher proportions of protein-like and microbially produced SOM and was relatively enriched in carbohydrates (17%) and carbonyl (9%). Freshly produced substances, such as carbohydrates, have a large impact on the interactions between SOM and its surroundings since carbohydrates are highly labile and preferentially utilized for microbial degradation as opposed to more humified material (Wu et al., 2009; Gustafsson et al., 2014; Shi et al., 2016; Lu et al., 2017). The properties of SOM in the

coarser grained RBS and AQS were similar, although the composition of the SOM in RBS more

closely resembled that of the near surface SLT SOM with slightly higher proportions of more labile carbonyl and carbohydrates (9% and 9% respectively) relative to AQS (7% and 5%, respectively). In general, a substantial amount of SOM is comprised of aromatic and aliphatic compounds which serve as a prominent sorption material for DOM (Weber Jr et al., 1992; Chin et al., 1997; Chefetz et al., 2000; Chefetz, 2003; Tremblay et al., 2005; Tang & Weber, 2006; Lin et al., 2007; Sun et al., 2008) and Fe (Adhikari & Yang, 2015; Groeneveld et al., 2020). At the study site, a higher percentage of the SOM had aliphatic C–H functional groups in RBS, SLT, and AQS than in CLY (37%, 32%, 37%, 26%, respectively). In contrast, a lower percentage of the SOM had aromatic functional groups in RBS, SLT, and AQS than compared to CLY (40%, 38%, 47%, 65%, respectively). The assignment of the aliphatic and aromatic peaks in the FTIR spectra were further supported by the relationship between the Ar:Al and both the HIX (r = 0.78) and abs254 (r = 0.96), which indicate the degree of humification and aromaticity, respectively (Fig. S2) (Ohno, 2002; Weishaar et al., 2003; Zsolnay, 2003).

As humification proceeds over time, the degradation of more characteristic structures results in the enhancement of refractory signals from simpler aliphatic and aromatic compounds (Kelleher et al., 2006; Chefetz & Xing, 2009). In the FTIR spectra, the total area under peaks attributed to both aliphatic C–H chains and aromatic rings increased with depth (RBS < SLT < AQS < CLY, Table S2). This indicates increasing levels of humification with depth. Compared to more labile compounds (i.e., polysaccharides, proteins), aliphatic C–H chains and aromatics are relatively recalcitrant, yet these compounds contain a high sorption affinity and readily interact with mineral surfaces (Coward et al., 2018; Groeneveld et al., 2020). Similarly, long C–H chains are hydrophobic and accumulate in the SOM pool by adsorbing onto mineral surfaces, such as kaolinite (Lehmann et al., 2007; Nuzzo et al., 2020). Furthermore, in one study investigating the

stability of Fe-oxide-bound to OM, Adhikari and Yang (2015) found that Fe-oxides bound with aliphatic C–H are more resistant to reduction than Fe-oxides bound to aromatic structures, leading to the accumulation of aliphatic C–H chains in older pools of SOM. Nevertheless, the increase of humified SOM structures with depth observed in the present study (Fig. 3, Table 2) is consistent with the accumulation of humic-like and aromatic SOM in the shallow aquifer sediments of Bangladesh under reducing conditions (McArthur et al., 2004; Mladenov et al., 2010; Datta et al., 2011).

### 4.2 Contrasting influences of SOM on As and Fe mobility

455

456

457

458

459

460

461

462

463

464

465

466

467

468

469

470

471

472

473

474

475

476

477

As presented above, a notable observation is the contrasting distributions of functional groups in the SOM between the fine grain samples SLT and CLY. Previous studies have demonstrated a positive correlation between the solid-phase concentrations of SOM, As, and Fe in the reducing shallow aguifers of Bangladesh (Dowling et al., 2002; Harvey et al., 2002; Anawar et al., 2003; Stüben et al., 2003), and growing evidence suggests that OM leached or expelled from fine grain layers mobilizes As (Aziz et al., 2008; Planer-Friedrich et al., 2012; Erban et al., 2013; Smith et al., 2018; Xiao et al., 2021; Pathak et al., 2022a; Pathak et al., 2022b), even in relatively oxidized, low As pre-Holocene aquifers which underly clay layers (Mihajlov et al., 2020). Regardless, it is widely agreed that OM drives the redox reactions governing the microbially mediated release of As (Bauer & Blodau, 2006; Cui & Jing, 2019), yet some fractions of SOM may regulate As mobility through differing mechanisms depending on the specific chemical properties (Anawar et al., 2013). For example, OM may strongly adsorb onto the surface of positively charged Feminerals (Sharma et al., 2010; Mladenov et al., 2015), which may regulate As mobility by displacing any adsorbed As (Bauer & Blodau, 2009), or forming ternary As-Fe-OM complexes via cationic bridging (Redman et al., 2002; Liu et al., 2011; Mikutta & Kretzschmar, 2011; de

Oliveira et al., 2015; Liu et al., 2020b; Aftabtalab et al., 2022). Therefore, the mass fluxes of As between the solid- and dissolved-phases are driven by the interactions between various OM functional groups and Fe.

478

479

480

481

482

483

484

485

486

487

488

489

490

491

492

493

494

495

496

497

498

499

500

The peak at ~1400 cm<sup>-1</sup> in the FTIR spectra is commonly attributed to ligand exchange mechanisms associated with carboxylate-Fe bonds (Gu et al., 1994; Fu & Quan, 2006; Kaiser & Guggenberger, 2007; Oren & Chefetz, 2012; Liu et al., 2020a). Carboxyl groups in soil SOM are important mediators of ion exchange reactions to extract metal cations from the sediment and groundwater (Wu et al., 2009; Gustafsson et al., 2014; Shi et al., 2016; Lu et al., 2017). Thus, SOM with abundant carboxylate groups can act to sequester Fe-minerals in the soil (Curti et al., 2021; Wen et al., 2022). However, most carboxylic acid derivatives are water soluble across the pH ranges found in natural groundwater (6.5 - 8.5) (Fox et al., 2017), and comprise the majority of the complexing DOM in the porewaters rich in dissolved Fe (Curti et al., 2021; Liu et al., 2022). Specifically, aromatic OM containing a carboxyl group favors the formation of aqueous Fe-OM complexes and may generate higher dissolved Fe concentrations in groundwaters (Wu et al., 2019a). In the case of the Meghna riverbank and aquifer sediments, the proportions of aromatic carboxylate groups in the SOM increase with depth similar to the to the water extractable concentrations of As and Fe (Varner et al., 2022) (Fig. S4). The abundance of aromatic carboxylate groups in the CLY sample suggests that the SOM here may maintain elevated As concentrations in the groundwater by providing an ample source of carboxyl-rich OM to the aquifer that favors the formation of soluble As-Fe-OM complexes. This idea is consistent with previous findings suggesting that clay layers in the shallow aquifers of Bangladesh are a prominent source of the DOM that sustains As mobility (Mukherjee et al., 2007a; Mukherjee et al., 2007b; Guo et al., 2019; Mihajlov et al., 2020).

The SOM in the SLT contains relatively high proportions of polysaccharides (17%), which have the potential to be utilized as electron donors for heterotrophic microbial respiration under both aerobic and anoxic conditions (Zhang et al., 2019) and are often indicative of high levels of microbial activity (Laspidou & Rittmann, 2002; Omoike et al., 2004). Under reducing conditions, polysaccharides may drive the microbially mediated reduction of the OM-bearing Fe-oxides (Haider, 2021). The RBS, SLT, and AQS also contain higher proportions of carbonyl groups assigned to the peak at  $\sim 1650$  cm<sup>-1</sup> (8.9%, 9.2%, 7.2%, respectively) than the CLY (5.8%). This peak is typically attributed to the C=O stretch of carbonyl bonded to proteinaceous amine (amide I). The SOM in the SLT contains the highest proportions of carbonyl and contained the highest β:α values and proportions of peak T, indicating the presence of freshly produced proteinaceous material (Fig. 3, Table S3). In general, the higher proportions of carbonyl components in the RBS, SLT, and AQS support the biological activity that may promote the microbial reduction of Asbearing Fe-oxide minerals (McArthur et al., 2001; Glodowska et al., 2020; Qiao et al., 2020). Overall, the reactivity of SOM as it relates to As and Fe in the sediment can be summarized by the Ar:Al and the HIX (Fig. S4). The SOM with higher HIX is associated with elevated solidphase As (> 9 mg/kg) and water-extractable As concentrations (> 0.6 mg/kg) (Varner et al., 2022). In contrast, the Ar:Al is more closely related to the water-extractable Fe concentrations (Fig. S4). These findings are consistent with previous work which showed that humic-like OM is linked to elevated dissolved As content within the groundwaters of the Bengal basin (Vega et al., 2017; Kulkarni et al., 2018a). Elevated proportions of carbohydrate and carbonyl along with lower proportions of aliphatic CH and carboxyl groups indicate a fresher and more labile source of

carbon in the near-surface SLT sediment. In contrast, the deeper CLY sediment is rich in

carboxylic derivatives favoring the formation of soluble OM-Fe-As complexes. Comparing the

501

502

503

504

505

506

507

508

509

510

511

512

513

514

515

516

517

518

519

520

521

522

SOM properties between SLT and CLY suggests that not all fine grain layers in the shallow aquifers of Bangladesh contribute to As mobilization in the same way.

## 4.3 Impacts of SOM makeup on As mobility in hyporheic zone sediments

The extent of As enrichment in the Meghna River HZ has previously been shown to be influenced by the grain size of the surficial sediments; sandy sediments promote the surface water-groundwater mixing required for the precipitation of As-attenuating Fe-oxides but surficial riverbank silt or clay prohibits advective mixing thereby preventing the accumulation of solid-phase As (Jung et al., 2015). Fine grain sediments along the Red River in Vietnam found to generate a high As plume in the adjacent aquifer by contributing to the persistent reduction of reactive Fe-oxides within the riverbank sediments (Stahl et al., 2016; Wallis et al., 2020).

The influence of a shallow buried silt layer (3 - 7 m bgl) underlying riverbank sands has not been studied in relation to the occurrence of As enrichment in HZ sediments, although we hypothesize that the silt layer may limit surface water-groundwater mixing and also provide a source of labile SOM to drive reductive processes. This may explain the markedly lower solid-phase As concentrations in the HZ at this site (7 ± 2 mg/kg) (Varner et al., 2022) compared to other measurements within the Meghna River HZ which commonly exceeded 500 mg/kg (Datta et al., 2009; Jung et al., 2015; Berube et al., 2018). Together, the SOM properties of the HZ sediments (SLT and RBS) indicate young, labile SOM with higher electron donating capacities than the underlying aquifer sediments. This is shown by the high proportions of both carbohydrates (16.9%) and carbonyl groups (9.2%) in the SLT samples, which are elevated compared to both the RBS (8.6% and 8.9%, respectively) and to the underlying AQS (4.9% and 7.2%, respectively). Thus, the silt layer serves as a source of labile OM to the overlying HZ which promotes reducing

conditions, preventing the accumulation of Fe-oxides which are capable of attenuating As in the HZ sediment.

The analysis of SLT and RBS samples in this study indicated the presence of relatively higher amounts of labile SOM containing polysaccharide and amide functional groups. This finding is consistent with Varner et al. (2022) where the analysis of water extractable SOM showed the presence of protein-like fluorescence peaks indicative of freshly derived OM. Together, it is inferred that the labile SOM in SLT and RBS may fuel heterotrophic processes such as the microbially-mediated reductive dissolution of Fe-oxides. In another study at the same site, Kwak et al. (In Revision) found that the dissolved As and Fe concentrations in the riverbank porewaters increased along the flow path as the groundwater discharged towards the river, from 23 to 164  $\mu$ g/L and 12 to 1858  $\mu$ g/L, respectively. Furthermore, these authors found that the dissolved inorganic carbon (DIC) concentrations, produced from the oxidation of organic carbon, increased substantially towards the river. However, the dissolved electron donors (i.e. DOM) could not explain the increase in the dissolved inorganic carbon, further implicating the sediments as a source of organic matter to the riverbank porewaters.

In addition to the reduction of As-bearing Fe-oxides, the production of CO<sub>2</sub> from the oxidative respiration of the SOM dissolves in the porewaters to form carbonic acid and organic acids, which accelerate the rate of silicate weathering (Gaillardet et al., 1999; Hanor & Wendeborn, 2023). At two previously characterized sites along the Meghna River, silicate weathering driven by the oxidation of SOM underlying the seasonally inundated floodplain releases enough dissolved products (silica, phosphate, dissolved inorganic carbon) to substantially modify the ambient chemistry within the HZ in ways that may influence the specific interaction of As with Fe-oxides, and the crystallinity of those oxides (Jewell et al., 2023). Furthermore, silicate minerals themselves

have been suggested to be prominent hosts of solid-phase As in the Bengal basin sediments (Charlet et al., 2007; Masuda et al., 2012; Varner et al., 2023).

569

570

571

572

573

574

575

576

577

578

579

580

581

582

583

584

585

586

587

588

589

590

591

In contrast, the SOM in the CLY contains a more humified and recalcitrant pool of carboxylrich SOM with a tendency to form soluble As and Fe complexes. These soluble complexes may contribute to elevated dissolved As concentrations in the aguifer should the SOM be mobilized from the clay aquitard. Sands comprising the shallow aquifers (< 60 m) in the Bengal Basin host the highest concentrations of dissolved As and Fe (Nickson et al., 1998; Harvey et al., 2002; Huq et al., 2020), with dissolved As commonly exceeding 50 µg/L and ranging up to 900 µg/L along the Meghna River (van Geen et al., 2003). At our study site, the groundwater As concentrations ranged between 10 and 120 µg/L, increasing with depth towards the clay aquitard (Kwak et al., In Revision). Although the functional groups in DOM have not been evaluated at this study site, fulvic acid extracted from high As groundwater (8.3 m depth) in Ariahazar, ~12 km north of the site in this study, was characterized by Mladenov et al. (2015) and further described in Kulkarni et al. (2018b). The fulvic acid component of the DOM in these studies contained an Ar:Al ratio ranging between 0.22 and 0.64 and the aromatic functional groups were noted to promote both electron shuttling processes (Kulkarni et al., 2018b) and the formation of As-Fe-OM complexes (Mladenov et al., 2015). In comparison, a fulvic acid standard and a humic acid standard (i.e., Suwanee River) contains an Ar:Al ratio of 0.72 and 1.76, respectively (Thorn et al., 1989). At this site, the bulk SOM in AQS, comprising the As-contaminated aquifer, contains a Ar:Al ratio of 0.89 whereas the CLY contains a Ar:Al of 1.86. Given that As and Fe are maintained in solution through complexation with more soluble portions of humic-like, aromatic OM (Sharma et al., 2010; Liu et al., 2011; Wu et al., 2019b), the release of aromatic carboxylate-rich SOM from CLY may support the observed As and Fe concentrations in the deeper groundwater at this site.

Here, we show that the SOM in the riverbank HZ sediments, shallow buried silt, and the underlying aquifer sediments contain varying chemical reactivities which contribute to As mobility through differing mechanisms. To the author's knowledge, the molecular composition of SOM has not been previously characterized in the sediments along an aquifer-river interface of a tidally fluctuating river in the Bengal basin. However, the elevated proportions of energetic labile SOM in the SLT and the prominence of aromatic-carboxylate groups favoring complexation in the CLY show differences in the SOM composition of the fine-grained sediments in the shallow aquifers of the Bengal basin which affects As mobility through opposing mechanisms.

#### 5 Conclusion

This study characterized the chemical reactivity of SOM from the HZ sediments along the Meghna River, Bangladesh and an As contaminated aquifer adjacent to the river. The SOM in both the riverbank and aquifer sands was shown to have a similar terrestrial source containing both humic-like and fulvic-like signatures. Variations in the chemical composition of the SOM in the shallow silt and clay aquitard revealed a more recalcitrant and degraded SOM in the clay aquitard with a high aromatic carboxylate content. In contrast, the shallow silt layer at ~3 m bgl contained fresher, microbially produced SOM with higher proportions of amides and polysaccharide moieties. The carboxylate-rich clay aquitard may support As mobility by favoring the formation of soluble As-Fe-OM complexes, while the labile SOM in the aquifer silt may promote As mobilization by fueling the microbially mediated dissolution of As-bearing Fe-oxides.

Within the HZ, the SOM of the shallow buried silt layer may inhibit the accumulation of solidphase As. Higher proportions of labile OM in the shallow silt layer and riverbank sands support the microbially-mediated reductive dissolution of As-bearing Fe-oxides under reducing conditions, preventing the accumulation of solid-phase As. Should the reactive SOM in the silt layer contribute to the dissolved load of the discharging groundwater during the dry season, the production of Fe-oxides may be limited by the influx of reactive DOM. These findings suggest that the variable SOM characteristics along the Meghna River and its adjacent aquifer contain differing reactive properties that regulate the geochemical processes governing As and Fe mobility. This study contributes to our understanding of the contrasting roles that SOM may have on As mobility within both riverine aquifers and the HZ along the river water-groundwater interface.

### 6 Acknowledgements

We thank Mahmudul Hasan and Mesbah Uddin Bhuiyan from the University of Dhaka for their assistance in the field. We would like to thank Dr. Audrey Lamb and Joshua Sanders at UTSA for assisting with the lyophilization process and the Chemistry Department at UTSA for providing access to the FTIR instrument. Funding was provided to Peter S. Knappett, M. Bayani Cardenas, and Saugata Datta by the National Science Foundation Hydrologic Sciences grant numbers EAR-1852652, EAR-1852653, and EAR-1940772, respectively.

#### 7 Credit author statement

Thomas Varner: Conceptualization, Methodology, Validation, Formal analysis, Investigation, Data curation, Writing – original draft, Visualization. Harshad V. Kulkarni: Conceptualization, Methodology, Validation, Formal analysis, Investigation, Data curation, Writing – review & editing, Visualization, Supervision. Peter Knappett: Resources, Writing – review and editing, Project administration, Funding acquisition. Bayani Cardenas: Resources, Writing – review and editing, Project administration, Funding acquisition. Saugata Datta: Conceptualization, Resources, Writing – review and editing, Project administration, Supervision, Funding acquisition.

646

647

648

649

650 651

652 653

654

655

656 657

658 659

660

661

662

663

664

665

666

667

668

- Adhikari, D., & Yang, Y. (2015). Selective stabilization of aliphatic organic carbon by iron oxide. Sci. Rep., 5(1), 1-7.
- Aeschbacher, M., Sander, M., & Schwarzenbach, R. P. (2010). Novel electrochemical approach to assess the redox properties of humic substances. *Environ. Sci. Technol.*, 44(1), 87-93.
- Aftabtalab, A., Rinklebe, J., Shaheen, S. M., Niazi, N. K., Moreno-Jiménez, E., Schaller, J., & Knorr, K.-H. (2022). Review on the interactions of arsenic, iron (oxy)(hydr) oxides, and dissolved organic matter in soils, sediments, and groundwater in a ternary system. *Chemosphere*, 286, 131790.
  - Anawar, H. M., Akai, J., Komaki, K., Terao, H., Yoshioka, T., Ishizuka, T., Safiullah, S., & Kato, K. (2003). Geochemical occurrence of arsenic in groundwater of Bangladesh: sources and mobilization processes. *J. Geochem. Explor.*, 77(2-3), 109-131.
  - Anawar, H. M., Tareq, S. M., & Ahmed, G. (2013). Is organic matter a source or redox driver or both for arsenic release in groundwater? *Phys. Chem. Earth, Parts a/b/c*, 58, 49-56.
  - Ascough, P. L., Bird, M. I., Francis, S., & Lebl, T. (2011). Alkali extraction of archaeological and geological charcoal: evidence for diagenetic degradation and formation of humic acids. *J. Archaeol. Sci.*, 38(1), 69-78.
  - Aziz, Z., van Geen, A., Stute, M., Versteeg, R., Horneman, A., Zheng, Y., Goodbred, S., Steckler, M., Weinman, B., Gavrieli, I., Hoque, M. A., Shamsudduha, M., & Ahmed, K. M. (2008). Impact of local recharge on arsenic concentrations in shallow aquifers inferred from the electromagnetic conductivity of soils in Araihazar, Bangladesh. *Water Resources Research*, 44(7). <a href="https://doi.org/10.1029/2007wr006000">https://doi.org/10.1029/2007wr006000</a>
  - Bai, Y., Subdiaga, E., Haderlein, S. B., Knicker, H., & Kappler, A. (2020). High-pH and anoxic conditions during soil organic matter extraction increases its electron-exchange capacity and ability to stimulate microbial Fe (III) reduction by electron shuttling. *Biogeosciences*, 17(3), 683-698.
  - Batista, A. P. S., Teixeira, A. C. S., Cooper, W. J., & Cottrell, B. A. (2016). Correlating the chemical and spectroscopic characteristics of natural organic matter with the photodegradation of sulfamerazine. *Water Res.*, 93, 20-29.
  - Bauer, M., & Blodau, C. (2006). Mobilization of arsenic by dissolved organic matter from iron oxides, soils and sediments. *Sci. Total Environ.*, 354(2-3), 179-190.
  - Bauer, M., & Blodau, C. (2009). Arsenic distribution in the dissolved, colloidal and particulate size fraction of experimental solutions rich in dissolved organic matter and ferric iron. *Geochim. Cosmochim. Acta*, 73(3), 529-542.
- 670 Bellamy, L. (2013). *The infra-red spectra of complex molecules*. Springer Science & Business 671 Media.
- Berube, M. (2017). *Geochemical controls on arsenic release into groundwaters from sediments:*in relation to the natural reactive barrier Kansas State University].
- Berube, M., Jewell, K., Myers, K. D., Knappett, P. S., Shuai, P., Hossain, A., Lipsi, M., Hossain,
   S., Aitkenhead-Peterson, J., & Ahmed, K. (2018). The fate of arsenic in groundwater
   discharged to the Meghna River, Bangladesh. *Environ. Chem.*, 15, 29.
- BGS&DPHE. Arsenic Contamination of Groundwater in Bangladesh; British Geological Survey & Department of Public Health Engineering: London, UK, 2001; 630.
- Bhattacharya, P., Jacks, G., Jana, J., Sracek, A., Gustafsson, J., & Chatterjee, D. (2001). Geochemistry of the Holocene alluvial sediments of Bengal Delta Plain from West Bengal,

- India: implications on arsenic contamination in groundwater. *Groundwater arsenic contamination in the Bengal Delta Plain of Bangladesh*, 3084, 21-40.
- Bibi, M. H., Ahmed, F., & Ishiga, H. (2008). Geochemical study of arsenic concentrations in groundwater of the Meghna River Delta, Bangladesh. *J. Geochem. Explor.*, 97(2-3), 43-58.
- Borisover, M., Lordian, A., & Levy, G. J. (2012). Water-extractable soil organic matter characterization by chromophoric indicators: Effects of soil type and irrigation water quality. *Geoderma*, 179, 28-37.
- Burrows, R. M., Rutlidge, H., Bond, N. R., Eberhard, S. M., Auhl, A., Andersen, M. S., Valdez, D. G., & Kennard, M. J. (2017). High rates of organic carbon processing in the hyporheic zone of intermittent streams. *Scientific Reports*, 7(1), 13198.
- Bustin, R., & Guo, Y. (1999). Abrupt changes (jumps) in reflectance values and chemical compositions of artificial charcoals and inertinite in coals. *Int. J. Coal Geol.*, 38(3-4), 237-260.
- 695 Chalmers, J. M., & Griffiths, P. R. (2002). *Handbook of vibrational spectroscopy* (Vol. 4). Wiley.
- 696 Charette, M. A., & Sholkovitz, E. R. (2002). Oxidative precipitation of groundwater-derived 697 ferrous iron in the subterranean estuary of a coastal bay. *Geophys. Res. Lett.*, 29(10), 85-698 81-85-84.

701

- Charlet, L., Chakraborty, S., Appelo, C., Roman-Ross, G., Nath, B., Ansari, A., Lanson, M., Chatterjee, D., & Mallik, S. B. (2007). Chemodynamics of an arsenic "hotspot" in a West Bengal aquifer: a field and reactive transport modeling study. *Applied Geochemistry*, 22(7), 1273-1292.
- 703 Chefetz, B. (2003). Sorption of phenanthrene and atrazine by plant cuticular fractions. *Environ.* 704 *Toxicol. Chem.*, 22(10), 2492-2498.
- 705 Chefetz, B., Deshmukh, A. P., Hatcher, P. G., & Guthrie, E. A. (2000). Pyrene sorption by natural organic matter. *Environ. Sci. Technol.*, *34*(14), 2925-2930.
- 707 Chefetz, B., Hader, Y., & Chen, Y. (1998). Dissolved organic carbon fractions formed during 708 composting of municipal solid waste: properties and significance. *Acta Hydrochim*. 709 *Hydrobiol.*, 26(3), 172-179.
- 710 Chefetz, B., & Xing, B. (2009). Relative role of aliphatic and aromatic moieties as sorption domains for organic compounds: a review. *Environ. Sci. Technol.*, 43(6), 1680-1688.
- 712 Chen, W., & Yu, H.-Q. (2021). Advances in the characterization and monitoring of natural organic 713 matter using spectroscopic approaches. *Water Res.*, 190, 116759.
- 714 Chin, Y.-P., Aiken, G. R., & Danielsen, K. M. (1997). Binding of pyrene to aquatic and commercial humic substances: the role of molecular weight and aromaticity. *Environ. Sci. Technol.*, 31(6), 1630-1635.
- Coble, P. G., Del Castillo, C. E., & Avril, B. (1998). Distribution and optical properties of CDOM
   in the Arabian Sea during the 1995 Southwest Monsoon. *Deep-Sea Res. II: Top. Stud. Oceanogr.*, 45(10-11), 2195-2223.
- Coble, P. G., Lead, J., Baker, A., Reynolds, D. M., & Spencer, R. G. (2014). *Aquatic organic matter fluorescence*. Cambridge University Press.
- Coble, P. G., & Timperman, A. T. (1998). Fluorescence detection of proteins and amino acids in
   capillary electrophoresis using a post-column sheath flow reactor. *J. Chromatogr. A*,
   829(1-2), 309-315.

- Coward, E. K., Ohno, T., & Sparks, D. L. (2018). Direct evidence for temporal molecular fractionation of dissolved organic matter at the iron oxyhydroxide interface. *Environ. Sci. Technol.*, 53(2), 642-650.
- Cui, J., & Jing, C. (2019). A review of arsenic interfacial geochemistry in groundwater and the role of organic matter. *Ecotoxicol. Environ. Saf.*, 183, 109550.
- Curti, L., Moore, O. W., Babakhani, P., Xiao, K.-Q., Woulds, C., Bray, A. W., Fisher, B. J., Kazemian, M., Kaulich, B., & Peacock, C. L. (2021). Carboxyl-richness controls organic carbon preservation during coprecipitation with iron (oxyhydr) oxides in the natural environment. *Commun. Earth Environ.*, 2(1), 1-13.

735

736

737

738

739

740

741 742

743

744

745

746 747

748

752

753

754

755756

- Datta, S., Mailloux, B., Jung, H.-B., Hoque, M., Stute, M., Ahmed, K., & Zheng, Y. (2009). Redox trapping of arsenic during groundwater discharge in sediments from the Meghna riverbank in Bangladesh. *Proc. Natl. Acad. Sci.*, 106(40), 16930-16935.
- Datta, S., Neal, A. W., Mohajerin, T. J., Ocheltree, T., Rosenheim, B. E., White, C. D., & Johannesson, K. H. (2011). Perennial ponds are not an important source of water or dissolved organic matter to groundwaters with high arsenic concentrations in West Bengal, India. *Geophys. Res. Lett.*, 38(20).
- de Melo Benites, V., de Sá Mendonça, E., Schaefer, C. E. G., Novotny, E. H., Reis, E. L., & Ker, J. C. (2005). Properties of black soil humic acids from high altitude rocky complexes in Brazil. *Geoderma*, 127(1-2), 104-113.
- de Oliveira, L. K., Melo, C. A., Goveia, D., Lobo, F. A., Armienta Hernández, M. A., Fraceto, L. F., & Rosa, A. H. (2015). Adsorption/desorption of arsenic by tropical peat: influence of organic matter, iron and aluminium. *Environ. Technol.*, 36(2), 149-159.
- Deng, Y., & Dixon, J. B. (2002). Soil organic matter and organic-mineral interactions. In *Soil mineralogy with environmental applications* (Vol. 7, pp. 69-107).
- Dowling, C. B., Poreda, R. J., Basu, A. R., Peters, S. L., & Aggarwal, P. K. (2002). Geochemical study of arsenic release mechanisms in the Bengal Basin groundwater. *Water Resour. Res.*, 38(9), 12-11-12-18.
  - Erban, L. E., Gorelick, S. M., Zebker, H. A., & Fendorf, S. (2013). Release of arsenic to deep groundwater in the Mekong Delta, Vietnam, linked to pumping-induced land subsidence. *Proceedings of the National Academy of Sciences*, 110(34), 13751-13756.
  - Fellman, J. B., Hood, E., & Spencer, R. G. (2010). Fluorescence spectroscopy opens new windows into dissolved organic matter dynamics in freshwater ecosystems: A review. *Limnol. Oceanogr.*, 55(6), 2452-2462.
- Fernández-Getino, A., Hernández, Z., Buena, A. P., & Almendros, G. (2010). Assessment of the effects of environmental factors on humification processes by derivative infrared spectroscopy and discriminant analysis. *Geoderma*, 158(3-4), 225-232.
- Fiebig, D. M. (1995). Groundwater discharge and its contribution of dissolved organic carbon to an upland stream. *Arch. Hydrobiol.*, *134*(2), 129-155.
- Findlay, S., Sinsabaugh, R. L., Sobczak, W. V., & Hoostal, M. (2003). Metabolic and structural response of hyporheic microbial communities to variations in supply of dissolved organic matter. *Limnol. Oceanogr.*, 48(4), 1608-1617.
- Fischer, H., Kloep, F., Wilzcek, S., & Pusch, M. T. (2005). A river's liver–microbial processes within the hyporheic zone of a large lowland river. *Biogeochemistry*, 76(2), 349-371.
- Flanagan, S. V., Johnston, R. B., & Zheng, Y. (2012). Arsenic in tube well water in Bangladesh:
   health and economic impacts and implications for arsenic mitigation. *Bull. World Health Organ.*, 90, 839-846.

- Fox, P. M., Nico, P. S., Tfaily, M. M., Heckman, K., & Davis, J. A. (2017). Characterization of natural organic matter in low-carbon sediments: Extraction and analytical approaches. *Org. Geochem.*, 114, 12-22.
- Fu, H., & Quan, X. (2006). Complexes of fulvic acid on the surface of hematite, goethite, and akaganeite: FTIR observation. *Chemosphere*, *63*(3), 403-410.
- Fultz, L. M., Moore-Kucera, J., Calderón, F., & Acosta-Martínez, V. (2014). Using Fourier Transform Mid-Infrared Spectroscopy to Distinguish Soil Organic Matter Composition
   Dynamics in Aggregate Fractions of Two Agroecosystems. Soil Sci. Soc. Am. J., 78(6),
   1940-1948.
- Gaillardet, J., Dupré, B., Louvat, P., & Allegre, C. (1999). Global silicate weathering and CO2
   consumption rates deduced from the chemistry of large rivers. *Chemical Geology*, 159(1-4), 3-30.

784

785

786 787

788

789 790

791

792 793

797

798 799

800

801 802

803

- Glodowska, M., Stopelli, E., Schneider, M., Lightfoot, A., Rathi, B., Straub, D., Patzner, M., Duyen, V., Members, A. T., & Berg, M. (2020). Role of in situ natural organic matter in mobilizing As during microbial reduction of FeIII-mineral-bearing aquifer sediments from Hanoi (Vietnam). *Environ. Sci. Technol.*, *54*(7), 4149-4159.
- Goldman, J. H., Rounds, S. A., & Needoba, J. A. (2012). Applications of fluorescence spectroscopy for predicting percent wastewater in an urban stream. *Environ. Sci. Technol.*, 46(8), 4374-4381.
- Groeneveld, M., Catalán, N., Attermeyer, K., Hawkes, J., Einarsdóttir, K., Kothawala, D., Bergquist, J., & Tranvik, L. (2020). Selective adsorption of terrestrial dissolved organic matter to inorganic surfaces along a boreal inland water continuum. *J. Geophys. Res.: Biogeosci.*, 125(3), e2019JG005236.
- Gu, B., Schmitt, J., Chen, Z., Liang, L., & McCarthy, J. F. (1994). Adsorption and desorption of
   natural organic matter on iron oxide: mechanisms and models. *Environ. Sci. Technol.*,
   28(1), 38-46.
  - Guan, X.-H., Shang, C., & Chen, G.-H. (2006). Competitive adsorption of organic matter with phosphate on aluminum hydroxide. *J. Colloid Interface Sci.*, 296(1), 51-58.
    - Guggenberger, G., Zech, W., & Schulten, H.-R. (1994). Formation and mobilization pathways of dissolved organic matter: evidence from chemical structural studies of organic matter fractions in acid forest floor solutions. *Org. Geochem.*, 21(1), 51-66.
    - Guo, H., Li, X., Xiu, W., He, W., Cao, Y., Zhang, D., & Wang, A. (2019). Controls of organic matter bioreactivity on arsenic mobility in shallow aquifers of the Hetao Basin, PR China. *J. Hydrol.*, *571*, 448-459.
- Gustafsson, J. P. (2006). Arsenate adsorption to soils: Modelling the competition from humic substances. *Geoderma*, *136*(1-2), 320-330.
- Gustafsson, J. P., Persson, I., Oromieh, A. G., van Schaik, J. W., Sjöstedt, C., & Kleja, D. B. (2014). Chromium (III) complexation to natural organic matter: mechanisms and modeling. *Environ. Sci. Technol.*, 48(3), 1753-1761.
- Haider, K. (2021). Problems related to the humification processes in soils of temperate climates. In *Soil Biochem*. (pp. 55-94). CRC Press.
- Hanor, J. S., & Wendeborn, F. C. (2023). Origin of sodium bicarbonate groundwaters, Southern Hills Aquifer System, USA by silicate hydrolysis. *Applied Geochemistry*, *148*, 105512.
- Harvey, C., Ashfaque, K. N., Yu, W., Badruzzaman, A. B. M., Ali, M. A., Oates, P. M., Michael, H. A., Neumann, R. B., Beckie, R., Islam, S., & Ahmed, M. F. (2006). Groundwater

- dynamics and arsenic contamination in Bangladesh. *Chem. Geol.*, 228(1-3), 112-136. https://doi.org/10.1016/j.chemgeo.2005.11.025
- Harvey, C., Swartz, C. H., Badruzzaman, A., Keon-Blute, N., Yu, W., Ali, M. A., Jay, J., Beckie, R., Niedan, V., & Brabander, D. (2002). Arsenic mobility and groundwater extraction in Bangladesh. *Science*, 298(5598), 1602-1606.
- Hasan, M. A., Ahmed, K. M., Sracek, O., Bhattacharya, P., Von Broemssen, M., Broms, S., Fogelström, J., Mazumder, M. L., & Jacks, G. (2007). Arsenic in shallow groundwater of Bangladesh: investigations from three different physiographic settings. *Hydrogeol. J.*, 15(8), 1507-1522.
- Hay, M. B., & Myneni, S. C. (2007). Structural environments of carboxyl groups in natural organic molecules from terrestrial systems. Part 1: Infrared spectroscopy. *Geochim. Cosmochim. Acta.*, 71(14), 3518-3532.
- Hayes, M. H., MacCarthy, P., Malcolm, R. L., & Swift, R. S. (1989). Humic substances II.
- Haynes, R. (2005). Labile organic matter fractions as centralcomponents of the quality of agricultural soils: anoverview. *Adv. Agron.*, 5, 221-268.
  - Hoffmann, M., Mikutta, C., & Kretzschmar, R. (2013). Arsenite binding to natural organic matter: spectroscopic evidence for ligand exchange and ternary complex formation. *Environmental Science & Technology*, 47(21), 12165-12173.
  - Horneman, A., van Geen, A., Kent, D. V., Mathe, P., Zheng, Y., Dhar, R., O'connell, S., Hoque, M., Aziz, Z., & Shamsudduha, M. (2004). Decoupling of As and Fe release to Bangladesh groundwater under reducing conditions. Part I: Evidence from sediment profiles. *Geochim. Cosmochim. Acta*.
- 838 , *68*(17), 3459-3473.

833

834 835

836

837

846

847 848

849

850

851

852

853 854

855

- Huang, Y., Knappett, P. S., Berube, M., Datta, S., Cardenas, M. B., Rhodes, K. A., Dimova, N. T.,
   Choudhury, I., Ahmed, K. M., & van Geen, A. (2022). Mass fluxes of dissolved arsenic
   discharging to the Meghna River are sufficient to account for the mass of arsenic in
   riverbank sediments. J. Contam. Hydrol., 251, 104068.
- Huguet, A., Vacher, L., Relexans, S., Saubusse, S., Froidefond, J.-M., & Parlanti, E. (2009).
   Properties of fluorescent dissolved organic matter in the Gironde Estuary. *Org. Geochem.*,
   40(6), 706-719.
  - Huq, M. E., Fahad, S., Shao, Z., Sarven, M. S., Khan, I. A., Alam, M., Saeed, M., Ullah, H., Adnan, M., & Saud, S. (2020). Arsenic in a groundwater environment in Bangladesh: Occurrence and mobilization. *J. Environ. Manage.*, 262, 110318.
  - Ilani, T., Schulz, E., & Chefetz, B. (2005). Interactions of organic compounds with wastewater dissolved organic matter: role of hydrophobic fractions. *J. Environ. Qual.*, 34(2), 552-562.
  - Jewell, K., Myers, K. D., Lipsi, M., Hossain, S., Datta, S., Cardenas, M. B., Aitkenhead-Peterson, J., Varner, T., Kwak, K., & Raymond, A. (2023). Redox trapping of arsenic in hyporheic zones modified by silicate weathering beneath floodplains. *Applied Geochemistry*, 105831.
  - Jung, H. B., Bostick, B. C., & Zheng, Y. (2012). Field, experimental, and modeling study of arsenic partitioning across a redox transition in a Bangladesh aquifer. *Environ. Sci. Technol.*, 46(3), 1388-1395. <a href="https://doi.org/10.1021/es2032967">https://doi.org/10.1021/es2032967</a>
- Jung, H. B., Zheng, Y., Rahman, M. W., Rahman, M. M., & Ahmed, K. M. (2015). Redox Zonation and Oscillation in the Hyporheic Zone of the Ganges-Brahmaputra-Meghna Delta: Implications for the Fate of Groundwater Arsenic during Discharge. *Appl. Geochem.*, *63*, 647-660. https://doi.org/10.1016/j.apgeochem.2015.09.001

- Kaiser, K., & Guggenberger, G. (2007). Sorptive stabilization of organic matter by microporous goethite: sorption into small pores vs. surface complexation. *Eur. J. Soil Sci.*, *58*(1), 45-59.
- Kelleher, B. P., Simpson, M. J., & Simpson, A. J. (2006). Assessing the fate and transformation of plant residues in the terrestrial environment using HR-MAS NMR spectroscopy. *Geochim. Cosmochim. Acta.*, 70(16), 4080-4094.
- Kobayashi, T., & Sumida, H. (2015). Effects of humic acids on the sorption and bioavailability of pyrene and 1, 2-dihydroxynaphthalene. *Soil Sci. Plant Nutr.*, *61*(sup1), 113-122.
- Kulkarni, H. V., Mladenov, N., Datta, S., & Chatterjee, D. (2018a). Influence of monsoonal recharge on arsenic and dissolved organic matter in the Holocene and Pleistocene aquifers of the Bengal Basin. *Sci. Total Environ.*, 637, 588-599.

872

873

874

875

876

883

884

885

886

887

888

889

- Kulkarni, H. V., Mladenov, N., Johannesson, K. H., & Datta, S. (2017). Contrasting dissolved organic matter quality in groundwater in Holocene and Pleistocene aquifers and implications for influencing arsenic mobility. *Appl. Geochem.*, 77, 194-205.
- Kulkarni, H. V., Mladenov, N., McKnight, D. M., Zheng, Y., Kirk, M. F., & Nemergut, D. R. (2018b). Dissolved fulvic acids from a high arsenic aquifer shuttle electrons to enhance microbial iron reduction. *Sci. Total Environ.*, *615*, 1390-1395.
- Kwak, K., Varner, T. S., Nguyen, W., Kulkarni, H. V., Buskirk, R., Pedrazas, M. N., Huang, Y.,
  Arman, A. S., Hosain, A., Aitkenhead-Peterson, J., Ahmed, K. M., Akhter, S. H., Cardenas,
  M. B., Datta, S., & Knappett, P. S. K. (In Revision). Surficial Sediment of Fluctuating
  Rivers are Hotspots for Arsenic Contamination.
- Laspidou, C. S., & Rittmann, B. E. (2002). A unified theory for extracellular polymeric substances, soluble microbial products, and active and inert biomass. *Water Res.*, *36*(11), 2711-2720.
  - Lee, D., & Seo, J. (2014). Three-dimensionally networked graphene hydroxide with giant pores and its application in supercapacitors. *Sci. Rep.*, 4(1), 1-6.
  - Lehmann, J., Kinyangi, J., & Solomon, D. (2007). Organic matter stabilization in soil microaggregates: implications from spatial heterogeneity of organic carbon contents and carbon forms. *Biogeochemistry*, 85, 45-57.
  - Li, K., Khanna, R., Zhang, J., Barati, M., Liu, Z., Xu, T., Yang, T., & Sahajwalla, V. (2015). Comprehensive investigation of various structural features of bituminous coals using advanced analytical techniques. *Energy & Fuels*, 29(11), 7178-7189.
- Lin, D., Pan, B., Zhu, L., & Xing, B. (2007). Characterization and phenanthrene sorption of tea leaf powders. *J. Agric. Food Chem.*, *55*(14), 5718-5724.
- Lin, V. S. (2015). Research highlights: challenges in the characterization, storage, and isolation of natural organic matter. *Environ. Sci.: Process. Impacts*, *17*(12), 2002-2005.
- Litvin, V. A., & Minaev, B. F. (2013). Spectroscopy study of silver nanoparticles fabrication using synthetic humic substances and their antimicrobial activity. *Spectrochim. Acta A: Mol. Biomol.*, 108, 115-122.
- Liu, G., Fernandez, A., & Cai, Y. (2011). Complexation of arsenite with humic acid in the presence of ferric iron. *Environ. Sci. Technol.*, 45(8), 3210-3216.
- Liu, K., Chen, Y., Xiao, N., Zheng, X., & Li, M. (2015). Effect of humic acids with different characteristics on fermentative short-chain fatty acids production from waste activated sludge. *Environ. Sci. Technol.*, 49(8), 4929-4936.
- Liu, R., Ma, T., Qiu, W., Du, Y., & Liu, Y. (2020a). Effects of Fe oxides on organic carbon variation in the evolution of clayey aquitard and environmental significance. *Sci. Total Environ.*, 701, 134776.

- Liu, W., Wang, Y., Li, J., Qian, K., & Xie, X. (2020b). Indices of the dual roles of OM as electron
   donor and complexing compound involved in As and Fe mobilization in aquifer systems
   of the Datong Basin. *Environ. Pollut.*, 262, 114305.
- Liu, X., Lu, J., Fang, X., Zhou, J., & Chen, Q. (2022). Complexation modelling and oxidation mechanism of organic pollutants in cotton pulp black liquor during iron salt precipitation and electrochemical treatment. *Chemosphere*, 308, 136374.
- Lu, J., Shi, Y., Ji, Y., Kong, D., & Huang, Q. (2017). Transformation of triclosan by laccase catalyzed oxidation: The influence of humic acid-metal binding process. *Environ. Pollut.*, 220, 1418-1423.
- Lumsdon, D. G., & Fraser, A. R. (2005). Infrared spectroscopic evidence supporting heterogeneous site binding models for humic substances. *Environ. Sci. Technol.*, 39(17), 6624-6631.
- Lv, J., Han, R., Huang, Z., Luo, L., Cao, D., & Zhang, S. (2018). Relationship between molecular components and reducing capacities of humic substances. *ACS Earth Space Chem.*, 2(4), 330-339.
- Macalady, D. L., & Walton-Day, K. (2011). Redox chemistry and natural organic matter (NOM):
   Geochemists' dream, analytical chemists' nightmare. In *Aquatic Redox Chemistry* (pp. 85-111). ACS Publications.
- MacCarthy, P., & Rice, J. A. (1985). Spectroscopic methods (other than NMR) for determining functionality in humic substances. In *Humic substances in soil, sediment and water* (pp. 527-559).
- Mailloux, B. J., Trembath-Reichert, E., Cheung, J., Watson, M., Stute, M., Freyer, G. A., Ferguson,
  A. S., Ahmed, K. M., Alam, M. J., Buchholz, B. A., Thomas, J., Layton, A. C., Zheng, Y.,
  Bostick, B. C., & van Geen, A. (2013). Advection of surface-derived organic carbon fuels
  microbial reduction in Bangladesh groundwater. *Proc. Natl. Acad. Sci.*, 110(14), 53315335. https://doi.org/10.1073/pnas.1213141110
- 932 Masuda, H., Shinoda, K., Okudaira, T., Takahashi, Y., & Noguchi, N. (2012). Chlorite—source 933 of arsenic groundwater pollution in the Holocene aquifer of Bangladesh. *Geochemical* 934 *Journal*, 46(5), 381-391.
- 935 Mayo, D. W., Miller, F. A., & Hannah, R. W. (2004). *Course notes on the interpretation of infrared*936 *and Raman spectra*. John Wiley & Sons.
- 937 McArthur, J., Banerjee, D., Hudson-Edwards, K., Mishra, R., Purohit, R., Ravenscroft, P., Cronin, 938 A., Howarth, R., Chatterjee, A., & Talukder, T. (2004). Natural organic matter in 939 sedimentary basins and its relation to arsenic in anoxic ground water: the example of West 940 Bengal and its worldwide implications. *Appl. Geochem.*, 19(8), 1255-1293.
- 941 McArthur, J., Ravenscroft, P., Safiulla, S., & Thirlwall, M. (2001). Arsenic in groundwater: testing 942 pollution mechanisms for sedimentary aquifers in Bangladesh. *Water Resour. Res.*, 37(1), 943 109-117.
- 944 McKnight, D. M., Boyer, E. W., Westerhoff, P. K., Doran, P. T., Kulbe, T., & Andersen, D. T. (2001). Spectrofluorometric characterization of dissolved organic matter for indication of precursor organic material and aromaticity. *Limnol. Oceanogr.*, 46(1), 38-48.
- 947 McManus, J., Heinen, E. A., & Baehr, M. M. (2003). Hypolimnetic oxidation rates in Lake 948 Superior: Role of dissolved organic material on the lake's carbon budget. *Limnol.* 949 Oceanogr., 48(4), 1624-1632.

- 950 Mecozzi, M., & Pietrantonio, E. (2006). Carbohydrates proteins and lipids in fulvic and humic 951 acids of sediments and its relationships with mucilaginous aggregates in the Italian seas. 952 *Mar. Chem.*, 101(1-2), 27-39.
- 953 Mihajlov, I., Mozumder, M. R. H., Bostick, B. C., Stute, M., Mailloux, B. J., Knappett, P. S., 954 Choudhury, I., Ahmed, K. M., Schlosser, P., & van Geen, A. (2020). Arsenic 955 contamination of Bangladesh aquifers exacerbated by clay layers. *Nat. Commun.*, *11*(1), 1-956 9.
- 957 Mikutta, C., & Kretzschmar, R. (2011). Spectroscopic evidence for ternary complex formation 958 between arsenate and ferric iron complexes of humic substances. *Environ. Sci. Technol.*, 959 45(22), 9550-9557.
- 960 Minor, E., & Stephens, B. (2008). Dissolved organic matter characteristics within the Lake Superior watershed. *Org. Geochem.*, 39(11), 1489-1501.
- 962 Minor, E. C., Swenson, M. M., Mattson, B. M., & Oyler, A. R. (2014). Structural characterization 963 of dissolved organic matter: a review of current techniques for isolation and analysis. 964 Environ. Sci.: Process. Impacts, 16(9), 2064-2079.

966

967

- Mladenov, N., Zheng, Y., Miller, M. P., Nemergut, D. R., Legg, T., Simone, B., Hageman, C., Rahman, M. M., Ahmed, K. M., & McKnight, D. M. (2010). Dissolved organic matter sources and consequences for iron and arsenic mobilization in Bangladesh aquifers. *Environ. Sci. Technol.*, 44(1), 123-128.
- Mladenov, N., Zheng, Y., Simone, B., Bilinski, T. M., McKnight, D. M., Nemergut, D., Radloff,
   K. A., Rahman, M. M., & Ahmed, K. M. (2015). Dissolved organic matter quality in a
   shallow aquifer of Bangladesh: implications for arsenic mobility. *Environ. Sci. Technol.*,
   49(18), 10815-10824.
- 973 Mukherjee, A., Fryar, A. E., & Howell, P. D. (2007a). Regional hydrostratigraphy and 974 groundwater flow modeling in the arsenic-affected areas of the western Bengal basin, West 975 Bengal, India. *Hydrogeol. J.*, 15(7), 1397-1418.
- 976 Mukherjee, A., Fryar, A. E., & Rowe, H. D. (2007b). Regional-scale stable isotopic signatures of recharge and deep groundwater in the arsenic affected areas of West Bengal, India. *J. Hydrol.*, 334(1-2), 151-161.
- 979 Mukherjee, A. B., & Bhattacharya, P. (2001). Arsenic in groundwater in the Bengal Delta Plain: 980 slow poisoning in Bangladesh. *Environmental Reviews*, *9*(3), 189-220.
- 981 Murphy, K. R., Stedmon, C. A., Graeber, D., & Bro, R. (2013). Fluorescence spectroscopy and multi-way techniques. PARAFAC. *Anal. Methods*, *5*(23), 6557-6566.
- Neumann, R. B., Ashfaque, K. N., Badruzzaman, A., Ali, M. A., Shoemaker, J. K., & Harvey, C.
   F. (2010). Anthropogenic influences on groundwater arsenic concentrations in Bangladesh.
   Nat. Geosci., 3(1), 46-52.
- Neumann, R. B., Pracht, L. E., Polizzotto, M. L., Badruzzaman, A. B. M., & Ali, M. A. (2014).
  Biodegradable organic carbon in sediments of an arsenic-contaminated aquifer in
  Bangladesh. *Environ. Sci. Technol. Letters*, 1(4), 221-225.
- Nickson, R., McArthur, J., Burgess, W., Ahmed, K. M., Ravenscroft, P., & Rahmanñ, M. (1998).

  Arsenic poisoning of Bangladesh groundwater. *Nature*, *395*(6700), 338-338.
- Nickson, R., McArthur, J., Ravenscroft, P., Burgess, W., & Ahmed, K. (2000). Mechanism of arsenic release to groundwater, Bangladesh and West Bengal. *Appl. Geochem.*, 15(4), 403-413.

- Nogaro, G., Datry, T., Mermillod-Blondin, F., Foulquier, A., & Montuelle, B. (2013). Influence of hyporheic zone characteristics on the structure and activity of microbial assemblages. *Freshw. Biol.*, 58(12), 2567-2583.
- Nuzzo, A., Buurman, P., Cozzolino, V., Spaccini, R., & Piccolo, A. (2020). Infrared spectra of soil organic matter under a primary vegetation sequence. *Chem. Biol. Technol. Agric.*, 7(1), 1-12.
- Ohno, T. (2002). Fluorescence inner-filtering correction for determining the humification index of dissolved organic matter. *Environ. Sci. Technol.*, *36*(4), 742-746.

- Olk, D., Brunetti, G., & Senesi, N. (2000). Decrease in humification of organic matter with intensified lowland rice cropping a wet chemical and spectroscopic investigation. *Soil Sci. Soc. Am. J.*, 64(4), 1337-1347.
- Omoike, A., Chorover, J., Kwon, K. D., & Kubicki, J. D. (2004). Adhesion of bacterial exopolymers to α-FeOOH: Inner-sphere complexation of phosphodiester groups. Langmuir, 20(25), 11108-11114.
- Oren, A., & Chefetz, B. (2012). Sorptive and desorptive fractionation of dissolved organic matter by mineral soil matrices. *J. Environ. Qual.*, 41(2), 526-533.
- Parlanti, E., Wörz, K., Geoffroy, L., & Lamotte, M. (2000). Dissolved organic matter fluorescence spectroscopy as a tool to estimate biological activity in a coastal zone submitted to anthropogenic inputs. *Org. Geochem.*, 31(12), 1765-1781.
- Pathak, P., Ghosh, P., Banerjee, S., Chatterjee, R., Muzakkira, N., Sikdar, P. K., Ghosal, U., Liang, M.-C., & Meeran, K. (2022a). Relic surface water (clay-pore water) input triggers arsenic release into the shallow groundwater of Bengal aquifers. *Journal of Earth System Science*, 131(2), 80.
- Pathak, P., Ghosh, P., Mukherjee, A., Ghosal, U., Liang, M.-C., Sikdar, P. K., & Kaushal, R. (2022b). Impact of differential surface water mixing on seasonal arsenic mobilization in shallow aquifers of Nadia district; western Bengal Basin, India. *Journal of Hydrology*, 612, 128270.
- Pedrazas, M. N., Cardenas, M. B., Hosain, A., Demir, C., Ahmed, K. M., Akhter, S. H., Wang, L., Datta, S., & Knappett, P. S. (2021). Application of electrical resistivity to map the stratigraphy and salinity of fluvio-deltaic aquifers: case studies from Bangladesh that reveal benefits and pitfalls. *Hydrogeol. J.*, 29(4), 1601-1610.
- Pettit, R. E. (2004). Organic matter, humus, humate, humic acid, fulvic acid and humin: their importance in soil fertility and plant health. *CTI Research*, 10, 1-7.
- Peuravuori, J., & Pihlaja, K. (2004). Preliminary study of lake dissolved organic matter in light of nanoscale supramolecular assembly. *Environ. Sci. Technol.*, *38*(22), 5958-5967.
- 1029 Piccolo, A. (1996). Humic substances in terrestrial ecosystems. Elsevier.
- Pike, P. R., Sworan, P. A., & Cabaniss, S. E. (1993). Quantitative aqueous attenuated total reflectance Fourier transform infrared spectroscopy: Part II. Integrated molar absorptivities of alkyl carboxylates. *Anal. Chim. Acta*, 280(2), 253-261.
- Ping, C., Michaelson, G., Dai, X., & Candler, R. (2001). Characterization of soil organic matter.

  In *Assessment methods for soil carbon* (pp. 273-283).
- Planer-Friedrich, B., Härtig, C., Lissner, H., Steinborn, J., Süß, E., Hassan, M. Q., Zahid, A., Alam, M., & Merkel, B. (2012). Organic carbon mobilization in a Bangladesh aquifer explained by seasonal monsoon-driven storativity changes. *Applied Geochemistry*, 27(12), 2324-2334.

- Qiao, W., Guo, H., He, C., Shi, Q., Xiu, W., & Zhao, B. (2020). Molecular evidence of arsenic mobility linked to biodegradable organic matter. *Environ. Sci. Technol.*, *54*(12), 7280-7290.
- Qu, S., & Cwiertny, D. M. (2013). Influence of organic surface coatings on the sorption of anticonvulsants on mineral surfaces. *Environ. Sci.: Process. Impacts*, 15(11), 2038-2049.
- Ravenscroft, P., Burgess, W. G., Ahmed, K. M., Burren, M., & Perrin, J. (2005). Arsenic in groundwater of the Bengal Basin, Bangladesh: Distribution, field relations, and hydrogeological setting. *Hydrogeol. J.*, 13(5), 727-751.
- Reddy, S. B., Nagaraja, M., Kadalli, G., & Champa, B. (2018). Fourier transform infrared (FTIR) spectroscopy of soil humic and fulvic acids extracted from paddy land use system. *Int. J. Curr. Microbiol. Appl. Sci*, 7, 834-837.
- Redman, A. D., Macalady, D. L., & Ahmann, D. (2002). Natural organic matter affects arsenic speciation and sorption onto hematite. *Environ. Sci. Technol.*, *36*(13), 2889-2896.

1056

1070

1071

- Riedel, T., Zak, D., Biester, H., & Dittmar, T. (2013). Iron traps terrestrially derived dissolved organic matter at redox interfaces. *Proc. Natl. Acad. Sci.*, 110(25), 10101-10105.
  - Ritter, K., Aiken, G., R, Ranville, J. F., Bauer, M., & Macalady, D. L. (2006). Evidence for the aquatic binding of arsenate by natural organic matter—suspended Fe (III). *Environmental Science & Technology*, 40(17), 5380-5387.
- Sánchez-Monedero, M. A., Cegarra, J., García, D., & Roig, A. (2002). Chemical and structural evolution of humic acids during organic waste composting. *Biodegradation*, 13(6), 361-371.
- Sandron, S., Rojas, A., Wilson, R., Davies, N. W., Haddad, P. R., Shellie, R. A., Nesterenko, P. N., Kelleher, B. P., & Paull, B. (2015). Chromatographic methods for the isolation, separation and characterisation of dissolved organic matter. *Environ. Sci.: Process. Impacts*, 17(9), 1531-1567.
- Schnitzer, M. (1983). Organic Matter Characterization. In *Methods of Soil Analysis: Part 2 Chemical and Microbiological Properties* (Vol. 9, pp. 581-594).
- Senesi, N., D'orazio, V., & Ricca, G. (2003). Humic acids in the first generation of EUROSOILS. *Geoderma*, 116(3-4), 325-344.
- Sharma, P., Ofner, J., & Kappler, A. (2010). Formation of binary and ternary colloids and dissolved complexes of organic matter, Fe and As. *Environ. Sci. Technol.*, *44*(12), 4479-4485.
  - Shi, Z., Wang, P., Peng, L., Lin, Z., & Dang, Z. (2016). Kinetics of heavy metal dissociation from natural organic matter: roles of the carboxylic and phenolic sites. *Environ. Sci. Technol.*, 50(19), 10476-10484.
- Shuai, P., Cardenas, M. B., Knappett, P. S. K., Bennett, P. C., & Neilson, B. T. (2017a).

  Denitrification in the banks of fluctuating rivers: The effects of river stage amplitude, sediment hydraulic conductivity and dispersivity, and ambient groundwater flow. *Water Resources Research*, 53(9), 7951-7967. <a href="https://doi.org/10.1002/2017wr020610">https://doi.org/10.1002/2017wr020610</a>
- 1077 Shuai, P., Knappett, P. S., Hossain, S., Hosain, A., Rhodes, K., Ahmed, K. M., & Cardenas, M. B.
  1078 (2017b). The impact of the degree of aquifer confinement and anisotropy on tidal pulse
  1079 propagation. *Groundwater*, 55(4), 519-531.
- Simeoni, M. A., Batts, B. D., & McRae, C. (2003). Effect of groundwater fulvic acid on the adsorption of arsenate by ferrihydrite and gibbsite. *Appl. Geochem.*, 18(10), 1507-1515.
- Smith, A. H., Lingas, E. O., & Rahman, M. (2000). Contamination of drinking-water by arsenic in Bangladesh: a public health emergency. *Bull. World Health Organ.*, 78, 1093-1103.

- Smith, R., Knight, R., & Fendorf, S. (2018). Overpumping leads to California groundwater arsenic threat. *Nature communications*, *9*(1), 2089.
- Stahl, M. O., Harvey, C. F., van Geen, A., Sun, J., Thi Kim Trang, P., Mai Lan, V., Mai Phuong, T., Hung Viet, P., & Bostick, B. C. (2016). River bank geomorphology controls groundwater arsenic concentrations in aquifers adjacent to the Red River, Hanoi Vietnam. Water Resour. Res., 52(8), 6321-6334.
- Stegen, J. C., Garayburu-Caruso, V. A., Danczak, R. E., Goldman, A. E., Renteria, L., Torgeson, J. M., & Hager, J. (2023). Maximum respiration rates in hyporheic zone sediments are primarily constrained by organic carbon concentration and secondarily by organic matter chemistry. *Biogeosciences*, 20(14), 2857-2867.
- Stevenson, F. J. (1994). Humus chemistry: genesis, composition, reactions. John Wiley & Sons.

1096

1097

1098

1099 1100

11011102

1103

1104

1105

1106

1107

1108 1109

1110

1111

- Stüben, D., Berner, Z., Chandrasekharam, D., & Karmakar, J. (2003). Arsenic enrichment in groundwater of West Bengal, India: geochemical evidence for mobilization of As under reducing conditions. *Appl. Geochem.*, 18(9), 1417-1434.
- Sun, K., Ran, Y., Yang, Y., & Xing, B. (2008). Sorption of phenanthrene by nonhydrolyzable organic matter from different size sediments. *Environ. Sci. Technol.*, 42(6), 1961-1966.
- Tang, J., & Weber, W. J. (2006). Development of engineered natural organic sorbents for environmental applications. 2. Sorption characteristics and capacities with respect to phenanthrene. *Environ. Sci. Technol.*, 40(5), 1657-1663.
- Tatzber, M., Stemmer, M., Spiegel, H., Katzlberger, C., Haberhauer, G., Mentler, A., & Gerzabek, M. H. (2007). FTIR-spectroscopic characterization of humic acids and humin fractions obtained by advanced NaOH, Na4P2O7, and Na2CO3 extraction procedures. *J. Plant. Nutr. Soil Sci.*, 170(4), 522-529.
- Thorn, K. A., Folan, D. W., & MacCarthy, P. Characterization of the International Humic Substances Society standard and reference fulvic and humic acids by solution state carbon-13 (13C) and hydrogen-1 (1H) nuclear magnetic resonance spectrometry; 1989; 1-93.
- Tremblay, L., Kohl, S. D., Rice, J. A., & Gagné, J.-P. (2005). Effects of temperature, salinity, and dissolved humic substances on the sorption of polycyclic aromatic hydrocarbons to estuarine particles. *Mar. Chem.*, 96(1-2), 21-34.
- van Geen, A., Ahmed, E. B., Pitcher, L., Mey, J. L., Ahsan, H., Graziano, J. H., & Ahmed, K. M. (2014). Comparison of two blanket surveys of arsenic in tubewells conducted 12 years apart in a 25 km(2) area of Bangladesh. *Sci. Total Environ.*, 488-489, 484-492. <a href="https://doi.org/10.1016/j.scitotenv.2013.12.049">https://doi.org/10.1016/j.scitotenv.2013.12.049</a>
- van Geen, A., Zheng, Y., Versteeg, R., Stute, M., Horneman, A., Dhar, R., Steckler, M., Gelman, A., Small, C., Ahsan, H., Graziano, J. H., Hussain, I., & Ahmed, K. M. (2003). Spatial variability of arsenic in 6000 tube wells in a 25 km2area of Bangladesh. *Water Resour. Res.*, 39(5). https://doi.org/10.1029/2002wr001617
- Varner, T. S., Kulkarni, H. V., Bhuiyan, M. U., Cardenas, M. B., Knappett, P. S., & Datta, S. (2023). Mineralogical Associations of Sedimentary Arsenic within a Contaminated Aquifer Determined through Thermal Treatment and Spectroscopy. *Minerals*, 13(7), 889.
- Varner, T. S., Kulkarni, H. V., Nguyen, W., Kwak, K., Cardenas, M. B., Knappett, P. S., Ojeda,
  A. S., Malina, N., Bhuiyan, M. U., & Ahmed, K. M. (2022). Contribution of sedimentary
  organic matter to arsenic mobilization along a potential natural reactive barrier (NRB) near
  a river: The Meghna river, Bangladesh. *Chemosphere*, 308, 136289.

- Vega, M. A., Kulkarni, H. V., Johannesson, K. H., Taylor, R. J., & Datta, S. (2020). Mobilization of co-occurring trace elements (CTEs) in arsenic contaminated aquifers in the Bengal basin. *Appl. Geochem.*, 122, 104709.
- Vega, M. A., Kulkarni, H. V., Mladenov, N., Johannesson, K., Hettiarachchi, G. M., Bhattacharya, P., Kumar, N., Weeks, J., Galkaduwa, M., & Datta, S. (2017). Biogeochemical controls on the release and accumulation of Mn and As in shallow aquifers, West Bengal, India. *Front. Environ. Sci.*, *5*, 29.
- Wallace, G. C., Sander, M., Chin, Y.-P., & Arnold, W. A. (2017). Quantifying the electron donating capacities of sulfide and dissolved organic matter in sediment pore waters of wetlands. *Environ. Sci.: Process. Impacts*, 19(5), 758-767.
- Wallis, I., Prommer, H., Berg, M., Siade, A. J., Sun, J., & Kipfer, R. (2020). The river–groundwater interface as a hotspot for arsenic release. *Nat. Geosci.*, *13*(4), 288-295.
- Wang, S., & Mulligan, C. N. (2006). Effect of natural organic matter on arsenic release from soils and sediments into groundwater. *Environ. Geochem. Health*, 28(3), 197-214.
- Weber Jr, W. J., McGinley, P. M., & Katz, L. E. (1992). A distributed reactivity model for sorption by soils and sediments. 1. Conceptual basis and equilibrium assessments. *Environ. Sci. Technol.*, 26(10), 1955-1962.
- Wei, J., Gao, B., Yue, Q., Wang, Y., Li, W., & Zhu, X. (2009). Comparison of coagulation behavior and floc structure characteristic of different polyferric-cationic polymer dual-coagulants in humic acid solution. *Water Res.*, 43(3), 724-732.
- Weinman, B., Goodbred, S. L., Zheng, Y., Aziz, Z., Steckler, M., van Geen, A., Singhvi, A. K., & Nagar, Y. C. (2008). Contributions of floodplain stratigraphy and evolution to the spatial patterns of groundwater arsenic in Araihazar, Bangladesh. *Bull. Geol. Soc. Am.*, 120(11-12), 1567-1580. <a href="https://doi.org/10.1130/b26209.1">https://doi.org/10.1130/b26209.1</a>
- Weishaar, J. L., Aiken, G. R., Bergamaschi, B. A., Fram, M. S., Fujii, R., & Mopper, K. (2003). Evaluation of specific ultraviolet absorbance as an indicator of the chemical composition and reactivity of dissolved organic carbon. *Environ. Sci. Technol.*, 37(20), 4702-4708.
- Wen, S., Lu, Y., Luo, C., An, S., Dai, J., Liu, Z., Zhong, J., & Du, Y. (2022). Adsorption of humic
   acids to lake sediments: Compositional fractionation, inhibitory effect of phosphate, and
   implications for lake eutrophication. *J. Hazard. Mater.*, 433, 128791.
- Wilson, H. F., & Xenopoulos, M. A. (2009). Effects of agricultural land use on the composition of fluvial dissolved organic matter. *Nat. Geosci.*, 2(1), 37-41.
- Wu, R., Li, H., & Cao, P. (2009). Amelioration of weathered coal on soil physical, chemical properties and enzyme activities with vegetation restoration. *J. Agro-Environ. Sci.*, 28(9), 1855-1861.
- Wu, X., Bowers, B., Kim, D., Lee, B., & Jun, Y.-S. (2019a). Dissolved organic matter affects arsenic mobility and iron (III)(hydr) oxide formation: implications for managed aquifer recharge. *Environmental Science & Technology*, 53(24), 14357-14367.
- Wu, X., Bowers, B., Kim, D., Lee, B., & Jun, Y.-S. (2019b). Dissolved organic matter affects arsenic mobility and iron (III)(hydr) oxide formation: implications for managed aquifer recharge. *Environ. Sci. Technol.*, *53*(24), 14357-14367.
- 1169 Xia, X., Teng, Y., & Zhai, Y. (2023). Influence of DOM and microbes on Fe biogeochemistry at a riverbank filtration site. *Environ. Res.*, *216*, 114430.
- 1171 Xiao, C., Ma, T., & Du, Y. (2021). Arsenic releasing mechanisms during clayey sediments compaction: An experiment study. *Journal of Hydrology*, 597, 125743.

- 1173 Xue, Q., Ran, Y., Tan, Y., Peacock, C. L., & Du, H. (2019). Arsenite and arsenate binding to ferrihydrite organo-mineral coprecipitate: Implications for arsenic mobility and fate in natural environments. *Chemosphere*, 224, 103-110.
- Yamashita, Y., & Tanoue, E. (2003). Chemical characterization of protein-like fluorophores in DOM in relation to aromatic amino acids. *Mar. Chem.*, 82(3-4), 255-271.
- Yu, W. H., Harvey, C. M., & Harvey, C. F. (2003). Arsenic in groundwater in Bangladesh: A geostatistical and epidemiological framework for evaluating health effects and potential remedies. *Water Resour. Res.*, 39(6).
- Zhang, X., Sun, Y., Ma, F., Li, A., Zhao, H.-p., Wang, A., & Yang, J. (2019). In-situ utilization of soluble microbial product (SMP) cooperated with enhancing SMP-dependent denitrification in aerobic-anoxic sequencing batch reactor. *Sci. Total Environ.*, 693, 133558.
- Zhao, Q., Gan, Y., Deng, Y., Zhou, H., & Zhao, H. (2022). Identifying carbon processing based
   on molecular differences between groundwater and water-extractable aquifer sediment
   dissolved organic matter in a Quaternary alluvial-lacustrine aquifer. *Applied Geochemistry*,
   105199.
- Zheng, Y., Stute, M., Van Geen, A., Gavrieli, I., Dhar, R., Simpson, H., Schlosser, P., & Ahmed,
   K. (2004). Redox control of arsenic mobilization in Bangladesh groundwater. *Appl. Geochem.*, 19(2), 201-214.
- Zhu, A., Yang, Z., Liang, Z., Gao, L., Li, R., Hou, L., Li, S., Xie, Z., Wu, Y., & Chen, J. (2020).
   Integrating hydrochemical and biological approaches to investigate the surface water and
   groundwater interactions in the hyporheic zone of the Liuxi River basin, southern China.
   J. Hydrol., 583, 124622.
- Zsolnay, Á. (2003). Dissolved organic matter: artefacts, definitions, and functions. *Geoderma*, 1197 113(3-4), 187-209.